Spontaneous Emergence of Static Friction Force and Vanishment of Dynamic Friction Force in Slip Front Propagation

*Takehito Suzuki[1], Hiroshi Matsukawa[1]

1.Department of Physics and Mathematics, Aoyama Gakuin University

We show spontaneous emergence of static friction force and vanishment of dynamic friction force in the dynamics of slip front propagation with local friction law nonlinearly depending on the slip velocity, which has no static friction force. We consider a block on a substrate and load one side of the block to slide it against the substrate. We take x axis along the loading direction and the block is assumed to be a semi-infinite isotropic homogeneous medium occupying the region $z>0$. The substrate is a rigid plane at $z=0$. The slip of block at x \to \infty is fixed to be zero and we load the block at x \to -\infty to initiate the slip. We employ the friction law having a quadratic form of the slip velocity, and derive the steady state solution for the motion of the slip front; the friction force tau is given by $-av^2 +2abv$, where v is the slip velocity and a and b are constants. With this friction law, the sliding friction force changes from the velocity-strengthening to the velocity-weakening behaviors with increasing slip velocity. This friction law enables us to treat the problem analytically, because the friction force is a single valued function of the slip velocity.
We can obtain the profiles of the slip and the strain of the steady state of the slip front dynamics, which is found to give the relationship between the strain at x \to -\infty (the loading point) p_{inf} (<0) and the slip front velocity c; $|p_{inf}|=2b/c$. It is also important to note that c must be smaller than the bulk elastic wave velocity v_e for the existence of the steady state. These statements indicate that p_{inf} has the critical value. If $|p_{inf}|<2b/v_e$, the steady propagation cannot be observed and the slip amplitude decays with increasing time. On the other hand, if $|p_{inf}|>2b/v_e$, the steady propagation of slip appears. These behaviors imply spontaneous emergence of the static friction force even though the local friction has no static friction force. Macroscopic static friction force is given by $2bE_1/v_e$, where E_1 is the Young modulus.
The analytical result obtained in the present study also indicates the slip velocity at $x_1(=x-ct)$ \to -\infty is $2b$, which results in that the friction force at the loading point in the steady state vanishes since tau is zero with $v=2b$. The dynamic friction force in the steady state is concluded to vanish spontaneously at x_1 \to -\infty.

Keywords: Static Friction Force, Dynamic Friction Force, Nonlinear Friction Law, Analytical Solution, Slip Front Propagation

An arithmetic approach for modeling of seismic activity, No.2

*Hiroyuki Fujiwara[1]

1.National Research Institute for Earth Science and Disaster Prevention

An arithmetic seismic activity model is proposed by Fujiwara (2014). In this model, earthquakes are modeled by using prime numbers to express the seismic activity that follows the G-R law. Although the arithmetic seismic activity model has been inferred from phenomenological similarities between seismic activities and the prime number distributions, there may be some mathematical and physical meanings behind the model.
We consider a correspondence between earthquakes and prime numbers. We parameterize occurrence time of earthquakes as prime numbers and magnitude of earthquakes as the interval of prime numbers. Then we obtain a relationship similar to G-R law. We call the model obtained from this correspondence as arithmetic seismic activity model. In the arithmetic seismic activity model, earthquake is equivalent to prime number. Then, earthquake prediction is equivalent to prediction of emergence of prime numbers.
For the prime number distribution, the Riemann explicit formula is known. The Riemann explicit formula is an equation showing the number of primes less than a given number, by using the zeros of the Riemann zeta function. In the arithmetic seismic activity model, the Riemann explicit formula gives a prediction formula of earthquake occurrence.

In this study, for the purpose of giving a physical interpretation to the arithmetic seismic activity model, efforts have been made in the following approach.
(1) By considering the Riemann explicit formula as a trace formula, we explore the mathematical structure behind it.
(2) Using the noncommutative geometry and automorphic representation, we challenge to build a dynamic system that can explain the arithmetic seismic activity model.

With respect to (1), the Selberg trace formula, which links geometry and harmonic analysis on a Riemann surface, is known. A common feature in the trace formula, the sum on the prime elements in the geometric side is equal to the sum on the eigenvalues in the spectrum side. Trace formula can be regarded as an equation linking the two different concepts. It is thought to play an important role in mathematical physical modeling. By paying attention to the similarity between the Selberg trace formula and the Riemann explicit formula and by capturing the Riemann explicit formula as a kind of trace formula, it was conducted a survey of the relevant existing research for mathematical structure behind the Riemann explicit formula.
With respect to (2), as a starting point of the above approach, focusing on the similarity between automorphic forms in the field of number theory and mathematical structure of the conformal field theory in the theoretical physics, we have been conducting research towards the construction of the dynamical system. By configuring the dynamical system based on the automorphic form and its representation in an adele space, we have been conducting preliminary research to capture earthquakes as an eigenvalue problem.
Approach of this study is to construct a bridge linking "prime" as a research subject of number theory and "earthquake" as a physical phenomenon. In the field of number theory, such attempt is known as Langlands program. In recent years, researches to expand the idea of the Langlands program between number theory and theoretical physics has been conducted.
For the prime distribution, historical unsolved problems, such as the Riemann hypothesis, still

exist in number theory. This study is still in the stage of preliminary research towards the resolution of the above-mentioned problems.

References

Hiroyuki Fujiwara (2014): An arithmetic seismic activity model, Zishin, vol. 66, 67-71.

Keywords: Number Theory, Prime number, Earthquake, Langlands program

Emergence and disappearance of repeating earthquakes on a geological fault in a deep gold mine in South Africa

*Junya Yamaguchi[1], Makoto Naoi[1], Masao Nakatani[2], Moriya Hirokazu[3], Thabang Kgarume[4], Toshihiro Igarashi[2], Osamu Murakami[5], Thabang Masakale[6], Yasuo Yabe[3], Kenshiro Otsuki[3], Hironori Kawakata[7], Tsuyoshi Ishida[1], Anthony Ward[8], Ray Durrheim[4,9], Hiroshi Ogasawara[7]

1. Kyoto University , 2.The University of Tokyo, 3.Tohoku University , 4.CSIR, 5.Tono Research Institute of Earthquake Science, 6.OHMS, 7.Ritsumeikan University, 8.SeismoGen, 9.University of the Witwatersrand, Johannesburg

We deployed an Acoustic Emission (AE) monitoring network consisting of 30 very sensitive AE sensors and 7 accelerometers at 1-km depth in the Cooke 4 gold mine in South Africa, where many earthquakes up to ~M 3 are induced by stress buildup by mining. Naoi et al. [2015] analyzed data obtained by the AE network during 2 months, and they found very small repeating earthquakes of $-5.1 \leq Mw \leq -3.6$ which occurred on a geological fault. In this study, we extended the analysis period to 14 months, investigating a time variation of the repeating earthquakes during longer periods.

Firstly, we relocated 5869 events that occurred along the geological fault during the 14 months (from 7 April 2011 to 30 may 2012) by using the double-difference method [Waldhauser and Ellsworth, 2000] with the cross-correlation travel-time reading technique. Of the relocated AEs, we chose 3735 events within 3 m from an approximation plane of the two-dimensional distribution of the AEs, which delineates the fault. We then cross-correlated waveforms of all event pairs whose interevent distances D were less than 2 m. We chose event pairs whose seismograms had cross-correlation coefficient greater than 0.90 at 20 percent or more working stations at the time and their rupture areas evaluated from a circular crack model overlapped significantly. We finally assembled them into “repeater groups” whose event pairs shared one event or more.Out of the 3735 events (35.6%), 1328 events belonging to 308 groups were identified as repeaters. The number of recurrence reached 45 times for the largest repeater group.

Activities of some groups continues for the whole 14 months (Type A), but we also found groups that newly emerged (Type B) or disappeared (Type C) in the analysis period. We also found areas of ~10-m scale where only Type-B or Type-C groups existed, which likely corresponds to a newly emerged or terminated macroscopic slow slip respectively. Meanwhile, there were areas where Type A-C existed within a tiny area of a-few-meter scale. Only in such area, we found some Type C groups whose events size decreased with time. We consider the emergence and disappearance of the repeaters in such areas represent formation and dissipation of unstable patches of the fault, resulting from newly encountered protruding portions or frictional wear of the contacts by the progress of fault creeping.

Keywords: Acoustic Emission, Induced Earthquake, Repeating Earthquake

Characteristics of Rupture Initiation and Propagation in the Lab

*Eiichi Fukuyama[1], Futoshi Yamashita[1], Shiqing Xu[1], Kazuo Mizoguchi[2,1], Shigeru Takizawa[1], Hironori Kawakata[3,1]

1.National Research Institute for Earth Science and Disaster Prevention, 2.Central Research Institute of Electric Power Industry, 3.Ritsumeikan Univ.

We have conducted large-scale bi-axial shear friction experiments using the NIED large-scale shaking table (e.g. Fukuyama et al., 2014, Yamashita et al., 2015). One of the main targets of these experiments was to investigate the rupture initiation and acceleration process of the stick slip events, which are proxies of natural earthquakes (hereafter, we call them labquakes). The experiments were done under constant loading rate conditions of between 0.01 and 0.1 mm/s under the normal stress of between 1.3 and 6.7 MPa. The rock sample is made of metagabbro from India. We compiled the results obtained in the series of experiments and discuss what we understood and what we need to understand. There are some key observations as follows. 1) We sometimes observed labquakes that did not reach the end of the rock sample. Such labquakes are more similar to the natural earthquakes in a sense that the total stiffness was controlled by the surrounding rock materials. In these events, highest stress drop occurred at the beginning while termination of the rupture was rather gradual. 2) Mainshocks were preceded by the precursory slow slip and/or foreshocks. Sometimes, foreshock activity dominates but in most cases, precursory slip occurred just before mainshocks. 3) The foreshocks tend to be more often observed when the sliding surface was pre-damaged due to previous fast sliding so that more gouge particles were generated under the same loading conditions. 4) After the friction experiment, many grooves were observed on the sliding surface, in which gouge particles were filled. The area where precursory slow slips occur does not have many grooves comparing to the other area, suggesting that slow slip might initiate mainly on the smooth surface where no grooves were created. 5) The hypocenters of the labquakes were located at the edge of the grooves based on the AE sensor array data. This suggests that grooves were created at the initial acceleration stage of the rupture. Based on the above observations, we are constructing the rupture model. And there are several issues that we do not clearly understand. a) Under what conditions, foreshock activity dominates? b) When gouge particles and grooves are created? c) Why precursory slip starts to occur at some point on the fault and expand to both slip perpendicular and slip parallel directions? These key questions will help to solve the rupture dynamics that occurred during the large-scale rock friction experiments.

Keywords: rupture propagation, friction experiments

Crustal deformation and Fault Model for the 2015 Nepal (Gorkha) Earthquake obtained from ALOS-2 SAR Interferometry data

*Tomokazu Kobayashi[1], Yu Morishita[1], Hiroshi Yarai[1]

1.GSI of Japan

A devastating earthquake with a moment magnitude (Mw) of 7.8 (USGS) struck central Nepal on April 25, 2015, with its hypocenter located in the Gorkha region. A Mw 7.3 aftershock occurred approximately 150 km east of the hypocenter of the main shock on 12 May 2015, which is the largest aftershock as of this writing. In this presentation, we report the detailed crustal deformation associated with these earthquakes obtained by InSAR analyses and the InSAR-inferred distributed slip model.

We employed a new Japanese L-band synthetic aperture radar satellite launched in 2014, called Advanced Land Observing Satellite-2 (ALOS-2), to measure the ground displacement. ALOS-2 possesses a ScanSAR mode which has an ability to observe over broad area with a swath width of 350 km in one action. The ScanSAR-based InSAR is indeed suitable for mapping the spatially comprehensive and detailed crustal deformation of the 2015 Gorkha earthquake.

We have successfully detected widely distributed ground displacements for the 2015 Gorkha earthquake by applying a ScanSAR-based interferometry analysis. A major displacement area extends with a length of about 160 km in the east-west direction. In the southern/northern part, the displacements moving toward/away from the satellite are observed in both orbits. The main crustal deformation area with ground displacement exceeding 1 m is located 20–30 km east from Kathmandu. A quasi-vertical displacement estimated by combining the ascending and the descending data indicates upheaval of about 1.4 m at maximum.

We inverted the InSAR data including both of the main shock and the largest aftershock to construct a slip distribution model. The fault geometry is assumed to be a plane fault. We set a rectangular fault with 220 km long and 150 km wide, corresponding to the plate interface between the Indian and the Eurasian plates. The fault is divided into square patches with a size of 10 x 10 km. The strike and the dip angles are set to be 290° and 10°, respectively. The major slip occurred with a maximum slip amount of approximately 6.3 m beneath the area 20-30 km northeast from Kathmandu, which is located in 80 km east-southeast of the hypocenter. No significant slip is identified further west from the hypocenter. The seismic rupture is thought to have propagated eastward unilaterally. The slips are nearly pure reverse fault motion, but on the deeper portion have a slight right-lateral component. The spatial extent is zonally distributed within a distance of 50 to 100 km from the surface along downdip direction. The downdip end of the slip is quite consistent with that of the interseismic coupling area geodetically inferred in previous studies. The total estimated moment magnitude including both the main shock and the Mw 7.3 event is 7.8 (seismic moment 7.0 x 10^{20} Nm). Inverting the InSAR data of pair Nos. 5 and 6 which are for the main shock only and the Mw 7.3 event only, respectively, the estimated moment magnitude is 7.8 (seismic moment 6.1 x 10^{20} Nm) and 7.3 (seismic moment 1.1 x 10^{20} Nm), respectively.

The slip distribution unnaturally bifurcates in the east, and we can identify a clear-cut slip deficit area with a radius of ~10 km just west side of the Mw 7.3 event. This area is presumably subjected to a strong shear stress which should promote a reverse fault slip. There is a possibility to produce a fault slip equivalent to Mw ~7.0 in the future although we do not know if the slip heterogeneity would be smoothed out by a seismic event or an aseismic event.

Acknowledgements: ALOS-2 data were provided from the Earthquake Working Group under a cooperative

research contract with JAXA (Japan Aerospace Exploration Agency). The ownership of ALOS-2 data belongs to JAXA. We used ASTER GDEM for the InSAR analyses and the topography mapping. ASTER GDEM is a product of METI (Ministry of Economy, Trade and Industry) and NASA.

Keywords: Crustal deformation, InSAR, Slip Distribution

Frictional properties of materials along Tohoku subduction plate boundaries and implications for fault motion

*Michiyo Sawai[1], André R Niemeijer[2], Takehiro Hirose[3], Christopher J Spiers[2]

1.Chiba University, 2.Utrecht University, 3.Kochi / JAMSTEC

The 2011 Tohoku-oki earthquake (Mw 9.0) nucleated at 24 km depth along the plate boundary. Moreover, episodic tremor and slow slip events occurred just before the 2011 Tohoku-oki earthquake on a shallow portion (less than 20 km depth) in the Tohoku subduction zone (e.g., Ito et al., 2013). The frictional properties of rocks composed of a subducting oceanic plate exert important controls on the various slip behavior from aseismic to seismogenic slip. However, frictional properties of the rocks to model such subduction earthquakes are poorly understood. We thus conducted friction experiments using a rotary shear apparatus on powders of blueschist (probably distributed at the Tohoku seismogenic zone) and smectite-rich pelagic sediments (present along the shallow portion of the Tohoku plate boundary (Chester et al 2013)). Experiments were performed at temperatures of 20-400°C, effective normal stresses of 25-200 MPa and pore fluid pressures of 25-200 MPa. We investigated the effects of temperature, effective normal stress and slip rate on the rate and state friction parameter (a-b) by conducting velocity-stepping experiments with velocity range from 0.1 to 100μm/s.

Blueschist gouges show a positive (a-b) values at 22°C which decrease to become negative with increasing temperature. At 200°C, the behavior is velocity weakening and shows negative (a-b) values. At 300ºC, the gouges show neutral to positive values of (a-b), showing larger (a-b) values than at 200ºC. (a-b) values slightly decrease again at 400°C. There is also effective normal stress dependence. The gouges exhibit a transition from velocity-strengthening to velocity-weakening with decreasing effective normal stress. Observed (a-b) values decrease with decreasing effective normal stress because of an increase in b with decreasing effective normal stress. Our results suggest that increasing pore pressure is a key factor for nucleating slip leading to both megathrust and slow earthquakes.

In the case of Smectite-rich pelagic sediments, the simulated gouges show negative values of (a-b) at low temperatures of 20-50°C, except at the highest slip rate of 0.1 mm/s, and neutral or slightly negative values of (a-b) at temperatures of 50-100°C. However, at temperature of >150°C the gouges show positive values of (a-b) under almost all velocity conditions tested. The trend of (a-b) seems to be identical with that of a, and b shows an inverse relationship with (a-b). Slow slip events are considered to be able to nucleate under conditions where (a-b) value is negative but close to zero. These conditions are met at temperatures of 50-100°C in our experiments, which is consistent with temperature conditions under which slow slip events occur along the plate boundary at the Japan Trench. The frictional properties of the pelagic sediments explain well the observed distributions of slow slip events in Tohoku subduction zone.

Periodic slow slip and megathrust zone earthquakes in northeastern Japan

*Naoki Uchida[1], Takeshi Iinuma[2], Robert Nadeau[3], Roland Bürgmann[3], Ryota Hino[1]

1.Graduate School of Science, Tohoku University, 2.Japan Agency for Marine-Earth Science and Technology, 3.University of California, Berkeley

Both aseismic and seismic slip accommodate relative motion across partially coupled plate boundary faults. In northeastern Japan, aseismic slip occurs in the form of decelerating afterslip following large interplate earthquakes and as relatively steady slip on uncoupled areas of the subduction thrust. Here we report on a new quasi-periodic slow-slip behavior that is widespread in the megathrust zone. The repeat intervals of the slow slip range from 1 to 6 years and often coincide with or precede clusters of large (M ≥5) earthquakes, including the M9 Tohoku-oki earthquake. The examination of the spatio-temporal distribution of small repeating earthquakes with respect to the M ≥5 earthquakes suggests that the slow-slip pulses trigger the M ≥5 seismicity. These results suggest that inherently periodic slow-slip events result in periodic stress perturbations and modulate the occurrence time of larger earthquakes. The periodicity in the slow-slip rate has the potential to help refine time-dependent earthquake forecasts.

Keywords: slow slip, repeating earthquakes, interplate earthquakes

Coseismic and postseismic deformation and a fault model of the 2014 Northern Nagano Prefecture Earthquake

*Hiroshi Yarai[1], Tomokazu Kobayashi[1], Yu Morishita[1], Mikio Tobita[1], Shinya Yamada[1]

1.Geospatial Information Authority of Japan

Coseismic deformation derived from the 2014 norther Nagano Prefecture earthquake (Mj6.7) was observed by GPS stations of the permanent GPS Earth Observation Network system (GEONET) and ALOS-2/PALSAR-2 interferometric SAR.
We used ALOS-2/PALSAR-2 data acquired by both right and left look direction from descending orbits and right look direction from ascending orbit. The interferograms suggest that fault motion of the earthquake has reverse dip slip with left-lateral motion on an east dipping plane. The most concentrated crustal deformation is located in the southern part of rupture area near epicenter of the mainshock, showing displacements toward to the satellite with ~1 m at the maximum. Clear displacement discontinuity is recognized along western margin of the large crustal deformation area, which is just on the Kamishiro fault.
We invert the InSAR results with GNSS data to construct slip distribution model of the earthquake. From fringe pattern of InSAR images, we assumed that a fault plane changes dip angle at 2 km depth, low dip angle shallower than 2 km and steep dip angle deeper than 2 km. Our preliminary model shows large (over 1 m) slip on southern part of shallower segment and moderate (~1 m) slip around hypocenter of the mainshock on deeper segment. Both segments demonstrate reverse dip slip with left-lateral motion. On the other hand, no significant slip is estimated on northern part of shallower segment.
Postseismic deformation was detected by GEONET and ALOS-2 InSAR.
Acknowledgements.
The PALSAR-2 data obtained by the ALOS-2 were provided by the Japan Aerospace Exploration Agency (JAXA) through the Agreement between GSI and JAXA. The ownership of PALSAR-2 data belongs to JAXA.

Keywords: 2014 Northern Nagano prefecture earthquake , ALOS-2, InSAR, coseismic deformation, postseismic deformation

3D branching fault simulation for dynamic rupture process of 2014 Northern Nagano Prefecture Earthquake

*Ryosuke Ando[1], Kazutoshi Imanishi[2]

1.Graduate School of Science, University of Tokyo, 2.National Institute of Advanced Industrial Science and Technology, GSJ

The 2014, M_w6.2, Northern Nagano Prefecture Earthquake broke the Kamishiro fault, which constitutes the northern end of the Itoigawa-Shizuoka tectonic line (ISTL). Associated with this earthquake, several characteristic phenomena indicate the complex configuration of this earthquake processes, as indicative of immaturity of the fault owing to low activity of ISTL at this end section. One of such is found in the surface ruptures, where the offsets were observed to be nearly 1 m for the southern half of the source area, while such surface ruptures were not identified for the northern half. This surface observation consists with the surface displacement distribution inferred from InSAR analysis, suggesting the large slip areas concentrated at near the ground surface on the southern half and at a deeper depth on the northern half, respectively. The surface break is suggested to be a temporally stable structure for a geomorphologic time scale overlapping preexisting fault scarps, and moreover, cumulative fault slip has found by trenching surveys. Another characteristic observation is that the first motion solution of the focal mechanism exhibits nearly pure strike slip faulting, while the centroid moment tensor does the reverse faulting with considerable a non-double couple component. The focal mechanisms of the foreshocks, aftershocks and the spatial distributions of them show the geometry of the source fault is composed of a dipping main-fault and a nearly vertical branch fault.
In this study, we consider this inferred complex fault geometry and carry out the fully dynamic 3 dimensional rupture simulation to understand the factors controlling the observed spatially and temporally heterogeneous features in the rupture process. We give the constraints of the applied stress based on the stress tensor inversion conducted for the focal mechanisms of small earthquake occurred in this region before this earthquake sequence; the maximum principle stress axis is determined to be horizontal oriented at ENE-WSW as the overall direction of the main-fault strike is nearly N-S. The determined stress ratio $(S_2-S_3)/(S_1-S_3)$ is also considered as a constraint together with the assumption of the vertical stress is in the lithostatic condition.
For the numerical simulation, we employed newly developed efficient algorithm for the 3D dynamic boundary integral equation method, called the First Domain Partitioning Method (FDPM) (Ando, 2016, submitted). This method allow us to fully consider the 3D fault geometry together with the ground free surface effect. Each run of the simulation is completed in a few minutes with 48 cores and 15 GB of memory for the following model size: element sizes ~0.5 km, number of elements ~2,000 and time steps ~ 400.
We performed a series of parameter studies over the stress states concerning its uncertainty in the dynamic rupture simulation. We found, under a certain range of parameter sets, the rupture initiated on the vertical branch fault and then propagated to the dipping main-fault. We further obtained the slip distribution, which is dominated by the strike slip component on the branch-fault and by the reverse components on the main-fault as expected from the orientations of the faults and the principle stresses. In these cases, the reverse faulting slip shows the maximum on the shallow part of the main-fault above the hypocenter, presenting the similarity with the emergence of the observed surface break. The vertical branch-fault existing below the main-fault on the foot wall side seems to contribute the large slip at a depth on the northern half of the source area.

Keywords: Northern Nagano Prefecture Earthquake, 3D fault geometry, Dynamic rupture propagation simulation

Verification of unstable sliding behavior during dehydration of clay minerals as elevated temperature

*Tatsuro Kubo[1], Ikuo Katayama[1]

1.Department of Earth and Planetary Systems Science Hiroshima University

Along plate boundary subduction thrusts, the transformation of smectite to illite within fault gouge at temperatures around 100 - 200 °C is one of the key mineralogical changes thought to control the updip limit of seismicity (Hyndman et al., 1997). Ikari et al. (2007) suggest that decreasing water content may contribute to transition from velocity-strengthening to velocity-weakening behavior. Although they analyzed the velocity dependence of clay materials over a wide range of normal stresses and estimated the effect of hydration state on friction properties, their friction experiments were performed with controlling its water content. In the fact that hydration state of clay minerals is possible to vary from moment to moment in nature, systematic studies to investigate the effect of dehydration and hydrate state on frictional properties with progression of a removal of water is rare. In this study, we focus on the effect of dehydration of water on the frictional properties of clay minerals, and compare the results during dehydration process undergoing.

For the friction experiments, starting materials we used are Ca-montmorillonite (CaMMT). The powder materials of clays were placed on the simulated fault surface and two side blocks were placed together to produce a double-direct shear configuration. Normal stress was applied via a hydraulic ram on the side block with 60 MPa, and then, shear stress was applied by advancing the central block downward at a constant velocity. The sample assembly was heated by an external furnace up to 400 °C that is monitored by thermocouples located in the central part of sample assembly. We started to elevate the temperature around the specimen at a constant heating rate of 1, 3, and 10 °C/min, reaching after steady-state friction at 5 mm deformed. Then, we observed friction behavior of CaMMT during dehydration as elevated temperature. Because of the limitation of total displacement to 20 mm in our assembly, we used different slip rate 0.6, 1.2, and 3.0 μm/s at a heating rate 1, 3, and 10 °C/min, respectively.

CaMMT gouge showed unique friction behavior development as elevated temperature at a heating rate of 10 °C/min, which is divided into three stages; friction coefficient decreased at relative low temperature (1), friction coefficient increased at middle temperature (2), and stick-slip behavior occurred at high temperature (3). Stick-slip behavior as elevated temperature implies to have a potential of velocity weakening behavior. However, observed stick-slip behavior occur at a temperature of 324 °C, which is extremely higher from a temperature range of occurring dehydration for CaMMT (100 - 200 °C). We also performed subsequent experiments that heat gouge layer more slowly, using other heating rate; 1 and 3 °C/min. CaMMT gouge at a heating rate 1 °C/min showed similar friction behavior development to that of development at 10 °C/min, divided into three stages as described above. However, the temperature that stick-slip behavior occur shifted to lower temperature, 193 °C. If temperature controlled frictional behavior, the temperature of staring to occur stick-slip behavior is independent of heating rate, and there could be the threshold of temperature starting to exhibit unstable sliding. The observed systematical shift suggest that these frictional behavior is not controlled by temperature, but progression of dehydration. Each friction stages are related to dehydration process, at a first stage friction coefficient decreased because of generation of pore pressure during dehydration. At a second stage, friction coefficient

increased because of a removal of interstitial water, and at a third stage stick-slip behavior occurred when stiffness of gouge layer satisfies a given relationship (Rabinowicz, 1956). Dehydration of clay minerals is intimately connected to friction behavior, and it may have a possibility to trigger seismic friction.

Keywords: effect of dehydration, friction property, clay minerals, elevated temperature, stick-slip

Triggering and driving mechanisms of earthquake swarm

*Teruo Yamashita[1]

1.Earthquake Research Institute, University of Tokyo

Earthquake swarms usually occur in volcanic areas, geothermal fields and oceanic ridges. Detailed seismological observations suggest that swarm activity is driven by the flow of fluid, at least, at an initial stage of activity (e.g.,Yukutake et al., 2011). Hence, it is believed that high-pressure fluids are involved in the generation of earthquake swarm. However, recent geodetic observations suggest a possibility that aseismically evolving fault drives earthquake swarm activity (e.g., Takada and Furuya, 2010). Aseismic slip is, however, known to be induced by the injection of high-pressure fluid (e.g., Scotti and Cornet, 1994), so that aseismic slip evolution may be related to the existence of high-pressure fluid. It will therefore be indispensable to assume high-pressure fluid in the modeling of earthquake swarm. We may be able to consider the following two contrasting models (models 1 and 2) for the triggering and driving of earthquake swarm if the medium is saturated with fluid. Substantial local pressurization of pore fluid is assumed in model 1. If the crustal stress is near a critical level, ruptures triggered by the fluid pressurization will soon begin unstable growth according to linear fracture mechanics. Such ruptures will be regarded as ordinary earthquakes. Hence, we will have to assume highly under-stressed media and long-sustained supply of high-pressure fluid in model 1. However, model 1 has a weakness that how aseismic slip evolution is coupled with swarm activity is not clear. Although we do not assume local pressurization of fluid or highly under-stressed media in model 2, the fault zone is assumed to be permeated with high-pressure fluid. In such model, we will have to introduce some mechanism to suppress the accelerated rupture growth. One of the mechanisms that have strong compatibility with the existence of high-pressure fluid will be slip-induced dilatancy coupled with fluid flow, which is introduced in model 2. If the slip-induced dilatancy plays a dominant role, we do not necessarily require the local pressurization of fluid to trigger earthquake swarm. What is required for the triggering is the occurrence of small-size seed event. Fluid pressure lowers suddenly in the slip zone concurrently with the occurrence of the seed event if the degree of slip-induced dilatancy is large enough. Since the decrease in the fluid pressure raises the friction, the seed crack does not begin the growth soon after the nucleation. However, the dilatancy induces the fluid inflow from the surrounding medium, which gradually elevates the fluid pressure in the slip zone. This can trigger and drive the aseismic extension of slip zone if the stress state is near a critical level. The rate of aseismic extension depends on the balance between the fluid inflow rate and degree of slip-induced dilatancy. Spatial heterogeneity in the degree of slip-induced dilatancy or fracture strength gives rise to small-scale dynamic events, which will be a model for seismic swarm activity. We theoretically study the generation mechanism of earthquake swarm, assuming model 2, in this study. We analyze quasi-static extension of 2D crack in a linear poroelastic medium saturated with fluid. The dilatancy is assumed to increase with the slip evolution. We assume near-critical stress state, Coulomb's friction coupled with the effective normal stress and Darcy's law for the fluid flow. Our calculation shows that the moment evolution is proportional to t**1/2 for any values of the model parameters, which contrasts with the classical solution for dynamic crack growth, which is proportional to t**2 (Kostrov, 1964), where t is time. The expansion rates of aseismic slip zone are larger for higher diffusivities and lower degree of dilatancy. If the slip-induced dilatancy is locally negligible, small-scale dynamic slip is triggered at the advancing edge of aseismic slip zone, which is regarded as the occurrence of seismic event.

Keywords: earthquake swarm, fluid, dilatancy

A Source Inversion Method with Realistic Error Model

*Amato Kasahara[1], Yuji Yagi[2]

1.Graduate School of Life and Environment Sciences, University of Tsukuba, 2.Faculty of Life and Environmental Sciences, University of Tsukuba

Use of a proper likelihood function through incorporation of modeling error and a realistic noise model are essential part of a source inversion analysis, because the shape of the likelihood function affects choice of hyperparameters, the maximum a posteriori (MAP) estimate and its uncertainty estimate. We propose an empirical Bayes method for kinematic linear source inversion with physically based modeling error and realistic noise covariance.
The colored noise effects have been incorporated into analyses of Interferometric Synthetic Aperture Rader (InSAR) and global navigation satellite system (GNSS) data. Recently, effects of colored noise for centroid moment tensor (CMT) inversion were also discussed. However, the colored noise effects were usually ignored in source inversion analyses. In the proposed method, a noise covariance matrix is constructed from continuous records before P arrivals and uncertainty of phase picking.
In earlier studies, both amplitude of noise and a weight of a priori information were treated as hyperparameters. In the proposed method, we reformulated the marginal likelihood function to use the known noise covariance matrix estimated from data before P arrivals and phase picking errors.
As we are not able to know the true Earth structure, the calculated Green's functions contain modeling error, and incorporation of the modeling error is unavoidable for the source inversion analysis. Preceding studies approximated effects of modeling error by additional multivariate Gaussian noise (model noise) for data. One of the advantages of the previous approach is its simplicity. As a posterior probability distribution should still be a multivariate normal distribution, MAP estimation and its uncertainty estimation are straightforward. However, even when assuming multivariate Gaussian error for the elements in the coefficient matrix, it is shown that the theoretical likelihood function is a skewed function and not a multivariate normal distribution function. Thus, the previous approach biases the MAP estimate and potentially affect choice of hyperparameters. We propose another approach, which does not use model noise approximation, to incorporate effects of modeling error into source inversion analysis. In the present approach, the Earth structure is assumed to be a random variable, which follows a known probability distribution. Then, the Earth structure is marginalized to obtain a posterior probability distribution of the source process. The proposed approach naturally incorporates associations of modeling errors for different type of data (e.g. seismic waveforms and surface displacements). As the marginalization is not analytically possible in most cases, we use a Monte-Carlo method and obtain the posterior probability distribution as a finite mixture of multivariate normal distributions. The MAP estimate is obtained by using a numerical optimization technique.

Keywords: Source inversion, Empirical Bayes method, Modeling error

Statstical Properties of the Olami-Feder-Christensen Model on the Complex Network

*Hiroki Tanaka[1], Takahiro Hatano[1]

1.Earthquake Research Institute, Tokyo University

As a statistical model of seismicity, Olami-Feder-Christensen (OFC) model, which is thought to represent the stress distribution on the fault plane, has been studied and found that the model reproduces statistical properties similar to the real earthquakes including Gutenberg-Richter law and Omori formula for aftershock sequence. In most cases, OFC model has been studied on two-dimensional lattice, and the system is uniform in the sense that the cells are under the same condition. On the other hand, it is well known that earthquakes occur spatially non-uniformly. Recent studies showed that the network constructed by connecting the epicenters of successive earthquakes behaves as a Barabasi-Albert (BA) type scale-free network. Therefore in this study we simply incorporate such a spatial non-uniformity by thinking the OFC model on BA scale-free network and examine the statistical properties. This model includes two parameters; one is for the model construction, and the other is the dissipation-rate between nodes during stress redistribution. We mainly study the dissipation-rate dependence of statistical properties.
As a result, it is found that the magnitude frequency obeys nearly power law as well as the GR law, regardless of the dissipation-rate. Furthermore, by changing the dissipation-rate, the statistical behavior varies and is roughly categorized into three types; (1) Mainshock-Aftershock, (2) Foreshock-Mainshock-Aftershock, and (3) Stationary sequences. Especially first two behaviors are similar to the characteristic intermittent-clustering behavior of earthquakes.
Characteristic feature of this model is that even if the node has largest degree, sometimes multiple-releases occur in one event. During such a large event (regarded as the mainshock) stress redistribution is repeated between large degree nodes and overwhelmingly many smaller nodes. Therefore, as almost all nodes in the network are involved in the mainshock, aftershocks in this model are not considered to be the events releasing the remaining stresses which are not released by the mainshock.
In order to understand the role of aftershocks in this model, we propose a roughness parameter, which is thought to reflect the non-uniformity of stresses on the network, to make clear the total behavior of OFC model. With this parameter we found that aftershocks are not thought to be the events in order to release remaining stress at the edge of the mainshock rupture zone, but to be the process that nodes interact and cooperate to return to a stable roughness level specific to the construction of the network.

Unexpectedly rapid decrease of meter-sized rock friction at high work rate

*Futoshi Yamashita[1], Eiichi Fukuyama[1], Kazuo Mizoguchi[2], Shigeru Takizawa[1], Shiqing Xu[1], Hironori Kawakata[3]

1.National Research Institute for Earth Science and Disaster Prevention, 2.Central Research Institute of Electric Power Industry, 3.Ritsumeikan University

We here report rapid decrease of meter-sized rock friction at high work rate revealed by large-scale biaxial experiments at NIED. In the experiments, we used a pair of meter-sized Indian metagabbro as specimens, whose contacting area was 1.5 m long and 0.1 m wide. The experimental conditions were normal stress up to 6.7 MPa and loading velocity up to 3 $\times 10^{-2}$ ms^{-1}. We confirmed the work rate dependency of rock friction as previously reported with centimeter-sized experiments (Di Toro *et al*., 2011, Nature), but further found that the meter-sized rock friction starts to decrease at a work rate of 10^{-1} $MJm^{-2}s^{-1}$, which is one order of magnitude smaller work rate (still high in absolute sense) than that of the centimeter-sized one. After each meter-sized experiment, we found localized damages (i.e. grooves) were generated on the fault surface and gouge materials were distributed in and around them. Especially, we often found heavily comminuted gouge in the grooves, which swelled up relative to the surrounding fault surface. Mechanical, visual and material observations suggest that slip-evolved stress heterogeneity on the fault accounts for the differences of frictional properties between meter and centimeter sizes. Based on these observations, we propose that slightly stress-concentrated areas pre-exist in which frictional slip produces more gouge than in areas outside, resulting in further stress concentrations at these areas. The overall shear stress on the fault is primarily sustained by the stress-concentrated areas that undergo a work rate higher than the average, so those areas should weaken more rapidly and cause the macroscopic frictional strength to decrease abruptly. To verify this idea, we conducted numerical simulations assuming that local friction follows the frictional properties observed on centimeter-sized rock specimens. The simulations reproduced the macroscopic frictional properties observed on the meter-sized rock specimens. This result suggests the rapid reduction of macroscopic frictional strength at the work rate lower than the expected one with centimeter-sized results should be taken into consideration, since such slip-evolved heterogeneity should be common in nature. Further details related to this presentation can be found in Yamashita *et al*. (2015, Nature).

Keywords: Rock friction, Scale dependence, Work rate

Detection of frictional heating on faults using Raman spectra of carbonaceous material

*Kohtaro Ujiie[1,2], Hiroki Tabata[1], Yui Kouketsu[3], Hiroyuki Kagi[4], Weiren Lin[5]

1.Graduate School of Life and Environmental Sciences, University of Tsukuba, 2.Research and Development Center for Ocean Drilling Science, Japan Agency for Marine-Earth Science and Technology, 3.Graduate School of Environmental Studies, Nagoya University, 4.Geochemical Laboratory, Graduate School of Science, University of Tokyo, 5.Kochi Institute for Core Sample Research, Japan Agency for Marine-Earth Science and Technology

The detection of frictional heating on faults is a key to assessing coseismic shear stress and frictional work during earthquakes. Raman spectra of carbonaceous material (RSCM) have been widely used as a geothermometer on sedimentary and metamorphic rocks. We examined whether RSCM can be useful to detect increased temperatures associated with frictional heating on faults. The studied fault rocks are a few millimeters-thick pseudotachylyte derived from chert, 10 cm-thick cataclasite marked by fragments of chert in the carbonaceous mudstone matrix, and ~1 mm-thick pseudotachylyte derived from argillaceous rock, which are distributed in the exhumed accretionary complexes in the Mino-Tamba and Shimanto Belts, Japan. The results indicate that the intensity ratio of D1 and D2 Raman bands (I_{D1}/I_{D2}) markedly increase in pseudotachylytes, while increased I_{D1}/I_{D2} is absent in the cataclasite. The increased I_{D1}/I_{D2} values in pseudotachylytes are considered to represent coal maturation associated with increased heating along the localized slipping zone of less than a few millimeters thick. The absence of increased I_{D1}/I_{D2} values in the cataclasite may reflect the restricted temperature rise, which is consistent with distributed shearing along the 10 cm-thick slipping zone. The I_{D1}/I_{D2} values are also increased in the chert within ~2 mm from the upper boundary of the pseudotachylyte and drop to the background level >2 mm away from the upper boundary. In contrast, the increased I_{D1}/I_{D2} values are not observed in the chert below the pseudotachylyte and the argillaceous rocks above and below the pseudotachylyte. The measurements of thermal properties suggest that coal maturation in the chert within ~2 mm from the upper boundary of the pseudotachylyte is attributed to the higher thermal diffusivity in the hanging wall chert relative to the footwall chert and the argillaceous rock. The increased I_{D1}/I_{D2} values in pseudotachylytes and the chert within ~2 mm from the upper boundary of the pseudotachylyte indicate that coal maturation can occur during short-lived thermal events such as frictional heating on faults. Therefore, RSCM is useful to detect frictional heating. However, the conventional RSCM geothermometer cannot apply for the estimation of peak temperature during frictional heating on faults, because the maximum temperature determined from the RSCM geothermometer is well below the minimum temperatures recorded in the pseudotachylytes. The reaction kinetics incorporating the effects of rapid heating is necessary to establish frictional heating thermometer on faults.

The estimation of redox state based on the fluid-deposited graphite and sulfide minerals in fault rocks

*Yoshihiro Nakamura[1], Madhusoodhan Satish-Kumar[2], Tsuyoshi Toyoshima[2]

1.Graduate School of Science and Technology, Niigata University, 2.Department of Geology, Faculty of Science, Niigata University

The redox state in fault rocks provide valuable information on the physicochemical properties related to the fluids during seismic activity (O'hara and Huggins, 2005). However, there are very few studies on direct clues for fluid activities obtained from fluid inclusion (Boullier et al. 2001) and estimation of fluid contents using micro-FTIR (Famin et al. 2008). It is usually difficult to distinguish between syngenetic and postgenetic fluid activities from altered and hydrated fault rocks and pseudotachylytes that indicate paleo-seismic activity (Kirkpatrick and Rowe 2013).
Here we focus on carbon- and sulfur-bearing minerals in fault zones in order to understand the dynamic changes of oxygen fugacity (fO_2) and sulfur fugacity (fS_2). The study area, located in the Hidaka metamorphic belt, Hokkaido, Japan, is a metasedimentary unit where cataclasites, ultracataclasites and two different types of pseudotachylytes; Pst I and Pst II are distributed. Pyrrhotite (N[FeS] = 0.92-0.94) + Kfs assemblage is found in Pst I matrix, whereas biotite microlite + Kfs assemblages with fluid deposited graphite is only found in Pst II matrix. The fluid deposited graphite is only observed in the Pst II matrix, which was generated at around 1200 degree C, and characterized by the breakdown of plagioclase and apatite. The carbon isotope composition of the fluid deposited graphite were between -18.2 and -25.4 permil, shifting the carbon isotope values of +2 ~ +3 permil from the metamorphic graphite in protolith, cataclasite and Pst I.
Our observations suggest that the graphite and sulfide minerals converted to COHS fluids by frictional melting, and then reprecipitate as secondary minerals under favorable fO_2-fS_2 environments. In order to assess the redox state, we attempt to estimate the P-T-fO_2-fS_2 phase diagram during frictional melting. The thermal decomposition of biotite coexisting with graphite and sulfide minerals are deduced as:
Annite in biotite + 3Pyrite + 1.5Graphite = Sanidine + 6Pyrrhotite + H_2O + 1.5 CO_2
The breakdown of biotite changes the redox state to the more oxidation state at ranges between delta FMQ +0.5 ~ + 3.0. Under a high-temperature condition (> 1200 degree C), biotite microlite + Kfs with fluid deposited graphite are usually observed instead of pyrrhotite in pseudotachylytes. This suggests the negative shift to biotite stability field by lowering fS_2 and fO_2. In addition, using the positive 2~3 permil shift by carbon isotope fractionation, the calculated xCO_2 (= CO_2 / CH_4 + CO_2) ranges between 0.12 and 0.03. The calculated fO_2 is evaluated between -21.6 and -22.0 log $_{10}$ units, suggesting the CH_4 dominant fluid based on the estimated ideal fluid mixing model. When the fluid composition encounters the graphite saturation surface in COH diagram by supersaturation, the fluid deposited graphite begins to precipitate with hydrous silicates such as hydroxyapatite and titanite, and shift the large carbon isotope fractionation by small fluctuation in xH_2O. Such precipitation model is in good agreement with the microtextural observations in pseudotachylyte matrix. The most important implication of our finding is that the redox state in both types of pseudotachylytes are controlled by graphite breakdown. Our finding of fluid deposited graphite in pseudotachylytes suggest that sediments can produce the COHS fluids by frictional melting and the graphite play as a reducing agent in fault rocks.
References: Boullier et al. (2001), JGR, 106, 21965-21977. Famin et al. (2008), EPSL, 265, 487-497. Kirkpatrick and Rowe, (2013), JSG, 52, 183-198. O'hara and Huggins (2005), CMP, 148, 602-614.

Keywords: Graphite, Stable carbon isotope , Pseudotachylyte, Redox state

Aftershock distribution and focal mechanisms of 2014 M_w5.4 Orkney earthquake, South Africa, by using underground seismic networks in gold mines

*Kazutoshi Imanishi[1], Hiroshi Ogasawara[2], Yasuo Yabe[3], Shigeki Horiuchi[4], Makoto OKUBO[5], Osamu Murakami[6]

1.Geological Survey of Japan, AIST, 2.Faculty of Science and Engineering, Ritsumeikan University, 3.Research Center for Prediction of Earthquakes and Volcanic Eruptions, Graduate School of Science, Tohoku University, 4.Home Seismometer Corporation, 5.National Science Cluster, Kochi University, 6.Tono Research Institute of Earthquake Science, Association for the Development of Earthquake Prediction

The M_w5.4 Orkney earthquake occurred on August 5, 2014, near Orkney town, South Africa. The mainshock and aftershocks were recorded by underground networks in gold mines, which are composed of 46 three-component geophones installed at 2-3 km depths. The sampling rate is 6 kHz. The observed waveforms have high signal-to-noise ratios and contain higher frequency components up to at least 1 kHz, which provide the opportunity for precise determination of aftershock distribution and source parameters. We determined hypocenters of 2000+ aftershocks by automatic earthquake location software from Home Seismometer Corp. (Horiuchi et al., 2011). Aftershocks distributed at depths from about 4 to 7 km forming a 8 km-long in the NNW-SSE direction. The distribution agrees with one of nodal planes of the mainshock focal mechanism, suggesting that the mainshock represents a left lateral strike-slip fault. Aftershock focal mechanisms were determined from P-wave polarity data as well as body wave amplitudes. As a preliminary analysis, we analyzed aftershocks with at least 15 P-wave polarities and obtained 137 well-determined solutions. Most of aftershocks show a pure strike-slip mechanism that is similar to the mainshock. We also found some aftershocks whose P- and T- axis deviates from the general trend and contain normal or reverse faulting components. These events seem to distribute at the middle and the north of the aftershock distribution, suggesting the existence of local stress heterogeneity. Further analysis of aftershocks is needed to elucidate whether the heterogeneity was caused by stress changes due to the mainshock and/or associated with locally formed pre-mainshock stress regime.
Acknowledgements. The seismic network used in this study is operated by Anglogold Ashanti and Open House Management Solutions. The data processing was performed by Institute of Mine Seismology. The data ownership belongs to Anglogold Ashanti.

Keywords: 2014 Mw5.4 Orkney earthquake , Gold mines, South africa, Aftershock distribution, Focal mechanism

Responses of Stick-Slip Oscillator to Periodically External Forces (2)

*Kazuro Hirahara[1]

1.Department of Geophysics, Earth and Planetary Sciences, Graduate School of Sciences, Kyoto University

There have so far been a large number of studies on statistical significance of periodicity and seasonality of seismic activities. Recently, some studies have proposed physical mechanisms causing such periodicity and seasonality. For example, the following studies have been executed: stress perturbation on faults causing some correlation between seismic activity and Earth-Ocean tide (Tsuruoka & Ohtake, 2002); correlation between activity of low frequency earthquakes and oceanic tide (Nakata et al.,2008) and proposal of its nonlinear response (Ide & Tanaka,2014); correlation between large earthquake activity and long-term lunar tide (8.85 years) and amplification mechanism of lunar tide(Tanaka,2014); seasonality of Nankai trough earthquake occurrences (Mogi,1969; Ohtake & Nakahara,1999) and correlation between long-term lunar tide (18.61 years) and their occurrences (Ide & Tanaka,2014). Recently, Uchida et al.(2016) reported the existences of 1-6 year periodicities of repeating earthquake activities on the Pacific plate interface and their triggering large earthquakes.

As stated above, there exist some periodicities of slip behaviors ranging from slow slips to large earthquakes. And earthquakes occurring on plate interfaces and inland faults have some rhythms of recurrence intervals called earthquake cycles and co-rupturing of some earthquakes. We may consider the former periodicities as responses of stick-slip oscillator to periodic forces such as earth and ocean tides, and the latter earthquake cycles as interaction of coupled stick-slip oscillators in asperities and the co-rupturing as synchronization of asperity ruptures. Following these ideas, I started to explore the possibility of constructing a new model of earthquake activities and cycles, by both employing earthquake cycle simulations following rate-state friction law and synchronization theory developed in non-linear sciences (e.g., Kuramoto,1984).

Sugiura et al.(2014) investigated synchronization of coupled stick-slip oscillators following rate-state friction. There have been, however, no studies on responses to external forces. Therefore, Hirahara (2015, SSJ Fall meeting) investigated the responses of 1 degree of freedom stick-slip oscillator to external forces. This talk is a follow-up report.

Hirahara (2015) found m:n synchronization phenomena, which is usually called as Devil's Staircase, in cases of applying periodic external stresses with the amplitudes of 1/10 and 1/100 relative to the whole stress changes in stick-slip cycles. Here, fe:fc=m:n (m and n are coprime integers) where fe and fc are frequencies of external force and simulated system, respectively. Earth and ocean tidal loading has stress with the amplitude of kPa-10kPa, and such loading may cause synchronization of SSE with small stress changes of several 100 kPa.

In this talk, I try to explain m:n synchronization and its synchronization width by employing simulated phase response curves. Then, I show the responses to external forces with not single but multiple frequencies, and also the responses to forces based on actual earth and ocean tidal models. Further, I report another interesting phenomena of non-synchronization, where the intervals of slip increasingly varies, especially in rage of the larger external periods outside of m:n synchronization. These phenomena may be related to the observed fluctuations of periodicity of earthquake activities and cycles.

Keywords: Stick-Slip Oscillator, Synchronization, Rhythm, External Force, Earthquake Cycle Simulation

Frictional properties of mafic metamorphic gouges: Implication for slow earthquakes along the Nankai Trough

*Ayumi S. Okamoto[1], André R. Niemeijer[2], Christopher J. Spiers[2], Toru Takeshita[1]

1.Graduate School of Science, Hokkaido University, 2.Faculty of Geosciences, Utrecht University

Both megathrust earthquakes and slow slip events have occurred at similar depth of ~30 km along the Nankai Trough, near southwest Japan. A convergent subduction boundary consists of kinds of materials such as sediments constituting an accretionary prism and mafic/ultra-mafic rock constituting crust and upper mantle. In order to understand the mechanisms relevant to subduction zone earthquakes, and to discuss the effect of physical conditions such as temperatures (T) and pore pressure ratio (λ), we need to know the mechanical properties of these rocks. In this study, we investigate frictional properties of mafic rocks constituting the oceanic crust. Note that the mafic rocks have been gradually and partially transformed to metamorphic rocks by metamorphism. The oceanic crust at the uppermost part of the Philippine Sea plate subducting along the Nankai Trough, might have been transformed by metamorphisms into prehnite-pumpellyite (PP), prehnite-actinolite (PA) and greenschist (GS) facies (~10-20 km depth) rocks, and epidote-blueschit (eBS), epidote-amphibolite (eAM) and GS facies (~20-30 km depth) rocks, based on the metamorphic facies diagram from Hacker *et al.* (2003) and the temperature-depth profile calculated by Yoshioka *et al.* (2013). Observation of natural deformation texture of GS and BS rocks shows that fined-grained actinolite (Act) and chlorite (Chl) mixture fills up a space between relatively coarse-grained amphibole, epidote, clinopyroxene and opaque minerals. These fined-grained aggregates are deformed to a large strain accommodated by coupled micro-fracturing and pressure solution. Other dominant minerals (e.g. epidote), however, seem to be little deformed, and behave as rigid bodies.
Based on the observation, mentioned above, we performed hydrothermal ring shear experiments using a mixture of actinolite (Act, ~85%) and chlorite (Chl, ~15%) at effective normal stresses (σ_n^{eff}) of 50-200 MPa, pore fluid pressures (P_f) of 50-200 MPa, T of 22.5-600°C, and sliding velocities (V) of 0.0003-0.1 mm/s. Our results show that the rate- and state-dependent friction parameter *(a-b)* is affected by both σ_n^{eff} and P_f at T = 200-400°C. At low velocity-step (e.g. 0.0003-0.001 mm/s), *(a-b)* shows negative at this temperature range, whereas it increases to positive with increasing V.
To extrapolate the results of the mechanical behaviors outside the experimental conditions, we quantify the effects of σ_n^{eff} and P_f on *(a-b)* in the lowest velocity-step from 0.0003 to 0.001 mm/s, using a multiple regression analysis. By applying the results of these empirical fits to the *P-T* conditions of the Nankai Trough, we demonstrate that a high $\lambda(P_f / (\sigma_n^{eff} + P_f)$, pore pressure ratio) above ~0.92-0.95 is needed for unstable, velocity-weakening behavior on Act + Chl gouge. However, since *(a-b)* increases with increasing V, unstable slip nucleating in a mixture of Act + Chl, can transition to stable sliding with increasing V, and stop without developing a huge rupture event. Act + Chl gouges therefore might have slipped at low velocity, resulting in slow earthquakes concentrating stress in adjacent undeformed bodies (i.e. asperities) of different assemblages and texture.

Keywords: metamorphic rock, oceanic crust, frictional behavior, Nankai Trough, amphibole, pore pressure ratio

Correlation between frictional properties and deformation textures in frictional experiments on the biogenic sediment collected from the oceanic plate offshore Costa Rica

*Yuka Namiki[1], Akito Tsutsumi[1]

1.Graduate School of Science, Kyoto University

Various seismic behaviors such as large earthquakes, episodic slow slip events, or silent earthquakes are observed in subduction zones. This variation likely reflects spatial variations in frictional properties along the seismogenic portion of plate-boundary megathrusts (e.g., Bilek and Lay, 1998). A number of studies revealed frictional properties of clay sediments collected from the Nankai Trough (e.g., Brown, 2003). However, available experimental data have been limited mostly to clayey subduction-zone materials. In this study, to reveal the frictional properties of the biogenic sediments, we performed a series of friction experiments on silicic to calcareous ooze. The samples tested in this study were collected at a reference site of offshore Costa Rica (Site U1381) during the IODP expedition 334 and 344.
Namiki et al. (2014) have shown that the frictional properties of the silicic to calcareous ooze were different from those of the clay sediments as the following: (1) the steady-state μvalues of the silicic to calcareous ooze are high, measuring 0.6 to 0.8; and (2) the μvalues of the silicic to calcareous ooze samples show negative velocity dependence of friction at velocities of 0.0028 to 0.28 mm/s and positive velocity dependence at velocities of 0.28 to 2.8 mm/s. The second property is important because velocity-weakening behavior implies potentially unstable fault motion.
To understand the mechanism of generating such characteristic frictional properties of the silicic to calcareous ooze, a series of friction experiments were performed on biogenic amorphous silica as an end-member component of the silicic to calcareous ooze. We dissolved calcite by acid treatment, and gained amorphous silica whose particle size and shape were similar to natural sediments. The biogenic amorphous silica shows the following frictional properties: (1) the steady-state μvalue is high, measuring ~0.6, and (2) the biogenic amorphous silica shows negative velocity dependence of friction at velocities of 0.0028 to 2.8 mm/s. The first property suggests the frictional steady-state strength of the biogenic amorphous silica is similar that of the silicic to calcareous ooze. The second property suggests mixing amorphous silica and calcite probably influences positive velocity dependence of friction of the silicic to calcareous ooze at velocities of several mm/s.
Microstructures of the sheared samples are observed by SEM. The silicic to calcareous ooze, which displays positive velocity dependence of friction at velocities of 0.28 to 2.8 mm/s, shows distributed deformation texture. The silicic and calcareous shells show preferred orientation inclined to the shear zone at an angle in the range of about 30°. Both distributed and localized deformation textures are observed for the amorphous silica sample, which shows negative velocity dependence of friction at velocities of 0.0028 to 2.8 mm/s. Preferred orientation of silica grains characterizes the distributed deformation textures. Two types of localized deformation textures are observed: zones of random fabric and shear fractures. In the random-fabric zones, silica grains are rounded. The rounded silica does not show the typical shape of the shells. The shear fractures intersect with the shear zone at an angle in the range of 10° to 20°. Preferred orientation of the silica grains parallel to the orientation of the shear fractures are observed within one of the shear fractures. Ikari et al. (2013) mentioned the nannofossil chalk, which showed negative velocity dependence of friction, exhibited prominent Riedel shears. It is likely that the localized deformation textures observed in our amorphous silica experiments are Riedel shears.

Keywords: Frictional experiments, Shear structure, CRISP

The effect of heterogeneous crust on earthquakes:a case study of the 2011 North Nagano earthquake

*Takashi Miyatake[1]

1.Earthquake Research Institute, University of Tokyo

We investigated the effects of heterogeneous crustal structure on earthquake rupture of the 2011 North Nagano earthquake. Using a 3D crustal structure model (Matsubara et al.,2008) we calculate stress distribution by solving static equation of motion. The finite difference method with grid size of 0.1km is used, where the computational space is 100km x 100km x 50km. Displacement boundary condition is applied. Since absolute value of boundary displacement is unknown, relative values of stress components, and the stress ratio, i.e., (fault shear stress) / (fault normal stress) are discussed. Because (stress ratio) = (stress drop) / (normal stress) −dynamic frictional coefficient, the ration roughly indicates normalized stress drop. We found high stress ratio region seem to be overlapped the fault asperity. It suggests that the earthquake could have been created by a heterogeneous stress field generated from heterogeneous crustal structure.

Keywords: crustal structure, fault stress, asperity

The Effective Stress Law at a Brittle-Plastic Transition: Analogue Experiments with Halite Gouge Layers

*Hiroyuki Noda[1], Miki Takahashi[2]

1.Japan Agency for Marine-Earth Science and Technology, 2.National Institute of Advanced Industrial Science and Technology

We investigated the effect of pore pressure P_f near the brittle-plastic transition (BPT) for a halite (NaCl) shear zone. Our series of precut friction experiments with a gas-medium apparatus with temperature T≤200°C, confining gas pressure P_c≤150 MPa, and P_f≤140 MPa revealed that a tanh connection between the brittle and plastic regimes works well even at elevated P_f, with a coefficient for P_f in an effective stress law αbeing unity. Plastic deformation around the real contacts independent of the mean stress results in α=1 regardless of the ratio of the real contact area A_r/A. The functional dependency of the shear strength on the effective normal stress may deviate from a linear dependency with increasing A_r/A. The present findings support a smooth transition in a hypothetical steady-state strength profile around a BPT, providing new insights in geologically obtained paleo-stress data in exhumed mylonitic shear zones.

Keywords: Effective stress law, Brittle-plastic transition, Friction experiment

Rupture process during the 2015 Illapel Chile earthquake: Zigzag-along-dip rupture episodes

*Ryo Okuwaki[1], Yuji Yagi[1]

1.Graduate School of Life and Environmental Sciences, University of Tsukuba

We constructed a seismic source model for the 2015 Mw 8.3 Illapel, Chile earthquake, which was carried out with the kinematic waveform inversion method adopting a novel inversion formulation that takes into account the uncertainty in Green's function, together with the hybrid backprojection (HBP) method enabling us to track the spatiotemporal distribution of high-frequency (0.3–2.0 Hz) sources at high resolution by using globally observed teleseismic P-waveforms. A maximum slip amounted to 10.4 m in the shallow part of the seismic source region centered 72 km northwest of the epicenter and generated a following tsunami inundated along the coast. In a gross sense, the rupture front propagated almost unilaterally northward from the hypocenter at less than 2 km/s, however in detail the spatiotemporal slip distribution also showed a complex rupture propagation pattern: two up-dip rupture propagation episodes, and the secondary rupture episode may have been triggered by the strong high-frequency radiation event at the down-dip edge of the seismic source region. High-frequency sources tended to be distributed at deeper parts of the slip area, a pattern also documented in other subduction-zone megathrust earthquakes that may reflect the heterogeneous distribution of fracture energy or stress drop along the fault. The weak excitation of high-frequency radiation at the termination of rupture may represent the gradual deceleration of rupture velocity at the transition zone of frictional property or stress state between the megathrust rupture zone and the swarm area.

Keywords: complex rupture process during megathrust earthquake, backprojection, kinematic waveform inversion

On the magnitude and heterogeneity of crustal stress

*Yoshihisa Iio[1]

1.Disater Prevention Research Institute, Kyoto University

The Magnitude of shear stress in the crust is one of the most important parameters in seismology, however, it has been unknown in a long time. We will infer it from dense seismic data, and further estimate theoretically whether the magnitude is large or small.

Keywords: crustal stress, heterogeneity, seiemogenic region

Variability in ETAS parameters depending on estimation algorithms

*Yuta Mitsui[1], Jun Kataoka[2]

1.Department of Geosciences, Shizuoka University, 2.Faculty of Science, Shizuoka University

The ETAS model (Ogata, 1988) allows us to estimate background seismicity \mu without aftershock effects from an earthquake sequence. As an interesting example, Llenos et al. (2009) showed that slow tectonic deformation truly increased the background seismicity \mu but did not correlate with the other ETAS parameters about aftershock productivity. Several studies such as Ide et al. (2013) expanded in application Kataoka and Mitsui (2015, JpGU) tested this concept for some regions around Japan, and obtained implications for magma intrusion beneath Mt. Fuji after the 2011 Tohoku Earthquake, slow slip events at subduction zones, and attenuation of slow slips after large earthquakes.

For the above parameter estimation, we used SASeis2006 by Ogata (2006). SASeis2006 adopted the DFP method, a kind of quasi-Newton method. However, Kasahara and Yagi (2015, SSJ) constructed a new estimation algorithm based on Newton method and showed a margin for improvement in SASeis2006 especially in terms of initial value dependence.

On the basis of this situation, this study introduce four estimation methods and examine the variability in the estimation results. Namely, we compare the estimation results from the same initial values: (1) downhill simplex method (2) conjugate gradient method (3) quasi-Newton method (BFGS method) with parameter constraints (all parameters are limited in a range of 0.01~10) (4) Newton method. We use earthquakes around Japan (M>2) in the JMA hypocenter catalogue. The time range is every one year in 1998~2014. The spatial range is around the source region of the 1993 southwest-off Hokkaido earthquake and the 2003 Tokachi-oki earthquake.

We find that the solutions do not converge in some cases, especially of SASeis2006 or the Newton method. Moreover, we obtain the following results: [1] Variability in the estimated value of \mu is relatively smaller. The ratio of the maximum value to the minimum value is at most 1.8 times. [2] Variability in the estimated values other than \mu are far larger. The ratio of the maximum value to the minimum value often reaches 10 times, or greater. [3] When comparing among the log-likelihood functions for the estimated parameters, the Newton method accounts for approximately 65% of the maximum likelihood. The conjugate gradient method and the downhill simplex method follows.

Keywords: Seismicity, ETAS model, Parameter estimation

Mutation('08/10,'14/10) of aftershock activity of the 2004 off Kii Peninsula E.q., and Stress structure around the Trough

*Hirofumi Mase[1]

1.none

(Please refer to the Fig.) Because mantle that heads eastward under Chugoku-district pushes the edge of the subducting slab under Kinki-district, the slab tries to creep up and turn to the right by lateral-fault type(1). Two seamounts in the near south of Nankai Trough concentrate this stress like stake. After the north side of the seamounts was destroyed by the earthquake in 2004, the route that power is transmitted to them changed from "from North" to "from Northwest"(2). The aftershocks which still continue at present should change from digestion of the one which was left without breaking by mainshock into something the pressure from the northwest causes. I studied the changes to time passing.
(short circuit in October,2008)A fluctuation occurred at the beginning of October,2008 (Fig.2,3). There were lots of shocks in front of the seamounts in the plane plan. Those seem to have rushed into the south including space between the seamounts. This space would increase in the pressure. I tied first 6 of October to the occurrence order and got a straight line in front of seamount EM. I call the power concentrating at two seamounts at the northwest-southeast direction the northwest compression force NWF(W),NWF(E). (before the main shock,the north compression force NF(W),NF(E))
The state that shocks formed a bend, stood and reached the limit can be judged by the section. NWF(W),NWF(E) produced the new stress-transfer-face which developed to the lower part.
(short circuit in October,2014)The 2nd time of fluctuation is the beginning of October,2014 (Fig.4,5,6). I attached the date of occurrence to something in October and tied something to march with a line (Fig.4). I assigned the number to something important in the occurrence order. The line(encircled number3-1-5-6) which develops in front of seamount EM and the line(encircled number2-4) issued from seamount WM and tries to cross at right angles at the overhead crossing showed. I call compression force about the latter(encircled number2-4) synthetic compression force SWF(W),SWF(E).
I think NF is 0 and the reaction SF decreases at present and NWF is biggest and the reaction SEF is increased at present. The powers work in two seamounts is SWF, resultant of SF,NWF,SEF(Fig.8). The surrounding ground supports a stake after all. Because the seamount gets reaction by its move from the bottom of the sea, the seamount delays to react upon the sudden change of force.
(below,Fig.7)After short circuit in October,2008(the 2nd, 3rd period) it increases in the pressure between the two seamounts, so the pressure rises more and causes destruction effectively at the direction where SWF(W) pushes seamount WM. This is the background where the stress-transfer-face(line,encircled number2-4) appeared, and SWF(W) and NWF(E) intersected with the overhead crossing (the 3rd period).
There is a comment that stress field in the plate in the focal region crosses at right angles mostly in the convergence (the northwest) direction(6). I think this caught the earthquake generating stress that SWF(W) causes.
(1)MASE/JpGU2014/SSS29-P10 (2)MASE/JpGU2015/SSS30-P01 (4)AIST/Visualization system for subsurface structures/all-Japan hypocenter catalog by the JMA/above M1 (5)JHOD,JCG/Seafloor Topography of the Plate Boundaries (6)JAMSTEC/Nakano,Hori/SSJ2014/A22-07/Tectonic background of the 2004 off the Kii Peninsula earthquakes

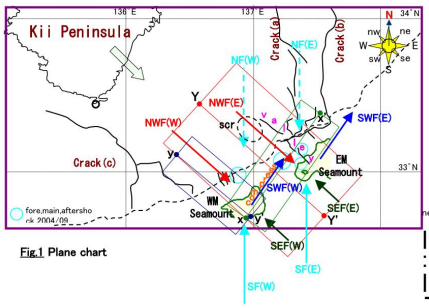

Fig.1 Plane chart

Stress which operates on Seamount

name	direction	size: until 2004/09	size: after 2004/09	cause of appearance
NF	from the north	biggest	0	edge of slave is repelled
SF	from the south	biggest	It decreases	reaction of NF
NWF	from the northwest	0	biggest	edge of slave is repelled
SEF	from the southeast	0	It increases	reaction of NWF
SWF	It's changing	—	It's changing	resultant of SF,NWF,SEF

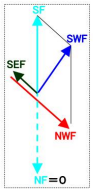

Fig.8

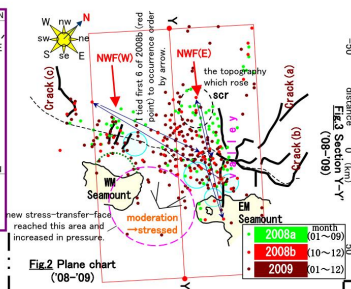

Fig.2 Plane chart ('08-'09)

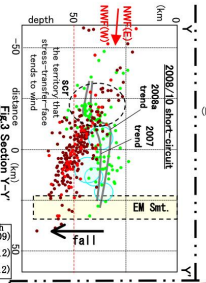

Fig.3 Section Y-Y' ('08-'09)

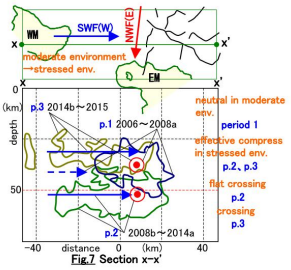

Fig.7 Section x-x'

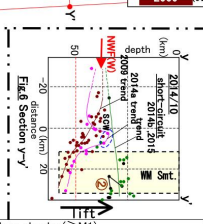

Fig.6 Section y-y'

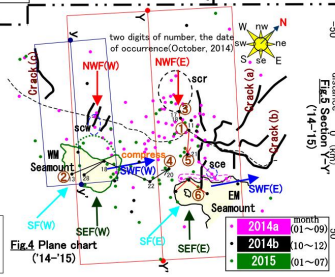

Fig.4 Plane chart ('14-'15)

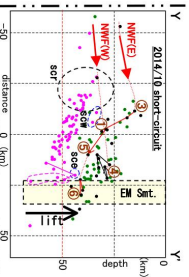

Fig.5 Section Y-Y' ('14-'15)

・small circles : shocks (≧M1) referable to (4)/shifted 10km to the southeast
・about sea bottom (shape line) extracted from (5)

Depth-dependent periodic change in the interplate coupling at NE Japan inferred from spatial gradient of velocity field

*Takeshi Iinuma[1]

1.Japan Agency for Marine-Earth Science and Technology

Surface velocity field of an island arc based on terrestrial GNSS observations includes the effect of the interplate coupling between the overriding continental plate to which the island arc belongs and oceanic plate that is subducting from a trench or a trough. In the Japanese Islands, many studies have been carried out to estimate the distribution of interplate coupling using the surface velocity fields based on the GNSS observations with a dense nationwide observation array [e.g., *Ito et al.*, 1999, 2000; *Mazzoti et al.*, 2000; *Nishimura et al.*, 2004; *Suwa et al.*, 2006; *Hashimoto et al.*, 2009; *Loveless and Meade*, 2010]. However, especially in northeast Japan, it is difficult to resolve the distribution of the interplate coupling along the direction normal to the Japan Trench based on the terrestrial geodetic data, because the trench where the subduction starts is too far (> 200 km) from the land. The spatial change in the degree of coupling is also hard to detect accurately far off the Pacific coast.
Uchida et al. [2016] revealed that the interplate coupling between the subducting Pacific and overriding continental plates at the northeast Japan subduction zone periodically changes with the repeat intervals from 1 to 6 years based on the analyses of the small repeating earthquakes and of surface displacement rate field. They applied a geodetic data processing for monitoring the spatio-temporal variation of interplate coupling with calculating the spatial gradient of the surface horizontal velocity field within belt-like zones that are taken along the direction perpendicular to the trench axis. Temporal change in the interplate coupling is detected with shifting the one-year time window in which the surface velocity field is estimated by one week, and spatial variation along the trench-parallel direction is deduced with shifting the latitude of the belt-like zone whose width is 60 km by 0.1 degree. They suggested that the gradient of the horizontal surface velocity depends mainly on the strength of the interplate coupling in shallow portion of the offshore plate interface, while it is still difficult to resolve the distribution of coupling zone on the plate interface and to estimate the temporal change in the degree of coupling in a quantitative manner.
The results of *Uchida et al.* [2016] with respect to the small repeating earthquakes implies that the spatial variation of repeating period of the slow slip on the plate interface depends on the depth, that is, the slow slip occurs with shorter recurrence interval at the deep portion than that at the shallow portion along each profile perpendicular to the trench. In this study, I examined the depth dependency of the repeating period of the slow slip on the plate interface by comparing the predominant periods of the temporal changes in the horizontal and vertical gradients of surface velocity field. *Iinuma et al.* [2010, 114th Meeting of the Geodetic Society of Japan] revealed that the sign of the vertical velocity gradient indicates the presence or absence of interplate coupling at deeper (>50 km) regions of the plate interface beneath the land. It means that the spatial gradient of the vertical velocity field is sensitive to the change in the interplate coupling at the deep portion, while the horizontal component is sensitive to the interplate coupling change at the shallow portion. The result of the examination shows that the predominant period of the temporal change in the vertical velocity gradient is shorter than that in the horizontal component at the most profiles. I will performing comprehensive numerical tests to examine the sensitivities of the spatial gradients of horizontal and vertical velocity fields to the interplate coupling at various depth ranges, and report the quantitative evaluation of the depth dependency of the cycle

of the periodic change in the interplate coupling.

Keywords: Interplate coupling, GPS, Northeast Japan, Slow slip event, mega-thrust earthquake, The 2011 off the Pacific coast of Tohoku earthquake

Spatial distribution of stress orientations in Southwestern Japan and its implication for the strength of the median tectonic line

*Keisuke Yoshida[1], Eiichi Fukuyama[1]

1.National research institute for earth science and disaster prevention

In Japan, many devastating earthquakes have historically occurred. There exist many active faults which may cause M>7 inland earthquakes in southwestern Japan. The Median Tectonic line (MTL) is one of the most active inland faults. Because of its large length, MTL has the potential to produce a very large earthquake. It is suggested from GPS analyses that steady aseismic slip at depth (>15 km) has continued to load shear stress on the shallower part of the fault plane of the MTL [Tabei et al., 2002]. In this study, we analyzed focal mechanism data to constrain stress and friction parameters of the MTL.
First of all, we determined focal mechanism solutions by using first-motion polarity data picked by Hi-net. We beforehand selected events with more than 15 first-motion polarity data, and searched acceptable nodal planes for each earthquake which can explain more than 90% of the first-motion data. We then omitted poorly-constrained focal mechanism of which RMS of acceptable nodal planes are more than 30°. As a result, we obtained 25,882 focal mechanisms data for the period between 2001 and 2015. This is 10 times as many as those listed in JMA catalogue. We then selected 14,460 focal mechanisms which occurred shallower than the plate boundary.
Next, we applied the stress tensor inversion method to this data set to investigate the detailed distribution of stress orientations. We first applied the stress tensor inversion developed by Michael [1987] to all the data. The estimated orientation of σ1-axis is WNW-ESE and the stress regime is strike-slip. This orientation largely differs from the orientations of the strain-rate and the relative plate movement as shown in previous studies [e.g. Wang, 2000]. One possible explanation is the effect caused by the collision between northeast and southwest Honshu. This stress orientation is unfavorably-oriented [Sibson, 1985] for the activation of the MTL.
Furthermore, we investigated the spatial distribution of stress orientations by using the following three approaches to subdivide the focal mechanisms catalogue: (a) employed a nonhierarchical clustering algorithm K-means,(b) assigned the focal mechanisms to each meshes with a 1.0° spacing, and (c) assigned the nearest 15-30 focal mechanisms to each grid node with a 0.1° spacing. In all cases,σ1-axes were estimated to be E-W in most of regions. However, the σ1-axes oriented NE-SW in the San-in region as shown in Kawanishi et al. [2009] based on the temporary seismic network data. This regions is situated highly strain concentration zone (Nishimura, 2014), and the orientations of stress is similar to that of the strain rate. Also, σ1-axis is oriented NW-SE in northern Shikoku. In this region, seismic activity is seen along the north-dipping MTL [Sato et al., 2015]. The focal mechanisms have a large diversity there. In Kii-Peninsula, the reverse fault stress regime was estimated. This distribution seems to correspond to the surface topography as seen in northeastern Japan [Yoshida et al., 2015]
The σ1-axes estimated along the MTL are oriented E-W, which are unfavorably-oriented for the reactivation on the MTL. We calculated the upper bound of the apparent frictional coefficient of the MTL to become easier to reactivate rather than form a new optimally oriented fault in intact crust. Estimated upper bound of the apparent frictional coefficient is less than 0.4 along most of the segments, which suggest the MTL is weak.

Keywords: The Median Tectonic line, stress, frictional strength, seismicity

Estimate of the stress state in earthquake source region in South African deep gold mine by DCDA

*Shuhei Abe[1], Yasuo Yabe[1], Takatoshi Ito[2], Masao Nakatani[3], Gerhard Hofmann[4], Hiroshi Ogasawara[5]

1.Research Center for Prediction of Earthquakes and Volcanic Eruptions, Graduate School of Science, Tohoku University, 2.Institute of Fluid Science, Tohoku University, 3.Earthquake Research Institute, the University of Tokyo, 4.Senior Mine Seismologist Rock Engineering, 5.Faculty of Science and Engineering, Ritsumeikan University

In the earthquake preparation process, the strength of a fault and the stress state around the fault evolve by interacting with each other through the fault slip. Therefore, many attempts have been done to measure the stresses around faults by deep drillings. However, techniques that are applicable to a large depth (> 1km) are limited. An earthquake of Mw2.2 (mainshock, hereafter) occurred at 3.3km depth in Mponeng mine, a deep gold mine in South Africa. The rupture plane of the mainshock diagonally cut a 30-m-thick gabbroic dike. Yabe et al. (2013) drilled a borehole passing the source fault of mainshock ~1.5 yrs afterward. They constrained possible ranges of the stress magnitudes, as well as the principal directions, based on the criteria of the borehole breakout and the core disking. In this study, we estimate the differential stress in a plane normal to the borehole axis with a higher resolution by Diametrical Core Deformation Analysis (DCDA, Funato and Ito, 2013) to the cores recovered from the borehole. DCDA is applied also to the cores of another borehole drilled ~7 mo before the mainshock in the same area. We also discuss applicability of DCDA to estimate stress at great depths.

DCDA estimates the differential stress from azimuthal variation in diameter (differential strain) of a core induced by stress relief associated with drilling. We collected seven core samples, ~30 cm long, from each borehole. The diameter was measured along circumferential profile lines set every ~2 cm on each core. Results: Coherent azimuthal variations in diameter were seen on three and five of seven core samples collected from the borehole drilled before and after the mainshock, respectively. Since core samples with incoherent diameter variations are considered to be damaged during drilling, we exclude them from the discussion below.

The pre-mainshock differential stresses were estimated to be ~100 MPa along the borehole from the central part of the dike to the host rock (quartzite) in west. The post-mainshock ones were about 20 MPa in the western host rock and near the west contact. On the other hand, it was ~70 MPa at the central part of the dike. The post-mainshock differential stresses obtained in this study fell in the range estimated by Yabe et al. (2013), while they were two times or more greater than their optimal values.

In DCDA, it is assumed that the core expansion induced by the stress relief by drilling is purely elastic. However, the core samples in this study were taken at a depth of ~3.3 km from the surface. The overburden pressure is as high as ~80 MPa. When such a high stress as ~80 MPa is unloaded, the inelastic deformation may occur, resulting in overestimation of the differential stress. In order to evaluate the effect of the inelasticity on the estimation, we carried out uniaxial creep tests of the dike. The ratio of the inelastic deformations to the elastic deformations was less than 10%. Just before the yielding under the uniaxial compression test or the uniaxial tensile (Brazilian) test, the inelastic strains were not larger than 30 % of the elastic strains. Therefore, the larger magnitudes of the differential stresses estimated in this study than those by Yabe et al. (2013) are not apparent by the inelasticity of the dike. There is a significant difference between the pre- and the post-mainshock differential stresses. However, because of different inclinations of the two boreholes, the pre- and the post-mainshock differential stresses cannot directly be

compared with each other. We grid-searched a stress state that can reproduce both differential stresses. The principal directions of stress were fixed to those by Yabe et al. (2013). The maximum magnitude of the principal stresses was 300 MPa. No stress state was found to simultaneously reproduce both of the pre- and the post-mainshock differential stresses, suggesting that DCDA can detect a temporal change in the stress state.

Keywords: South African deep gold mine, Diametrical Core Deformation Analysis

Searching largest displacement zone of the 2014 Orkney earthquake fault with strain data and using Map3Di for scientific drilling.

*Akimasa Ishida[1], Hiroshi Ogasawara[1], Hiroyuki Ogasawara[1], Taka Uchiura[1], Raymond Durrheim[2,3], Alex Milev[3], Makoto OKUBO[4], Teruhiro Yamaguchi[5]

1.Ritsumeikan University , 2.Univ. Witwatersrand, South Africa, 3.CSIR, South Africa,, 4.Kouchi University, 5.Hokkaidou University

The largest event recorded in a South African gold mining region, a M5.5 earthquake took place near Orkney on 5 August 2014. This is one of the rare events as the main- and after-shocks were recorded by 46 geophones at 2-3 km depths, 3 Ishii borehole strain meters at 2.9km depth, and 17 surface strong motion meters at close distances. The upper edge of the planar distribution of aftershock activity dipping almost vertically was only some hundred meters below the sites where the strainmeters were installed at distances larger than a few tens of meters from tunnel. A scientific project is planned to drill into the 2014 Orkney earthquake fault from the localities near the strain meter sites. It is a rare opportunity to recover fault material and fractures, to measure stress, to monitor after drilling at the M5.5 seismic zone.The final purpose of our research is to understand how main rupture stopped and why aftershock have occurred in sequence as observed. For this purpose, we attempted to constrain the largest displacement zone of the 2014 Orkney earthquake fault that account for the observed co-seismic strain with Map3Di to suggest where to drill. We checked polarities of each component of the strainmeters by comparing the observed tidal change with theoretically calculated tide Gotic2 [Sato and Honda (1984)], modifying the polarities of a few components with problems. Identical responses were recorded with the three strainmeters to a M4 earthquake at a few km distance, whereas .much larger (up to 1e-5) and different responses were recorded to the M5.5 earthquake.We calculated strain change of each component of the three strain meters by assuming uniform fault slip over a rectangle area with a same aspect ratio of aftershock area with various areas using map3Di. We found the rectangular area with a uniform fault slip of 0.5 m can explain the observed magnitudes of strain changes. However, we haven’t yet evaluated local effects that might cause discrepancies in each component of the three strainmeters. At Japan Geoscience Union Meeting 2016, we are going to make a follow-up report.

Keywords: South Africa, Boundary element method, Drilling project, Strain data, Seismogenic zones

Spatio-temporal variation of the stress drop revealed the generation and migration process of the 2009 swarm activity at Hakone volcano

*Miyu Fujioka[1], Yohei Yukutake[2], Ahyi KIM[1]

1.yokohama city university, 2.Hot Springs Research Institute of Kanagawa Prefecture

Hakone volcano has been an active volcano which is started about 400 thousands years ago. In addition the volcanic activity has caused seismic swarm periodically. Since those swarm activity occasionally generate widely felt earthquake, it is important to elucidate the generation process of the activity for future disaster mitigation. Yukutake et al. (2011) performed precise relocation of 2009 Hakone swarm hypocenters and found that a clear migration of the hypocenters which is consistent with diffusion of pressurized thermal fluid. However, it is still unclear 1) how the fluid controls the initiation of the swarm, and 2) whether all earthquakes during the sequence occurred under the same generation process.
In this study, to address the questions, we estimated the stress drop of the earthquakes observed during the 2009 sequence using empirical Green's function deconvolution method. Obtained stress drop were generally low, ranging between 0.01 MPa to 0.1 MPa, indicating the pore pressure increase might get involved the activity. Furthermore, the result showed the clear spatio-temporal variation of the stress drop: The stress drop tends to be higher when it occurs earlier and closer to the hypocenter of the initial earthquake. It implies that the flow of highly pressurized fluid initiated the swarm and promoted at the initial stage of seismic activity. However, at the middle to last stage, earthquakes might be triggered by pore pressure increase and/or stress perturbation due to the occurrence of the events earlier.

Keywords: Hakone volcano, swarm earthquakes, empirical Green's function method, stress drop, invaginated the fluid

Early rupture process of 14 March 2014 Iyo-Nada intermediate-depth earthquake inferred from 3D and 2D source imagings

*Takamasa Usami[1], Masanao Komatsu[1], Hiroshi Takenaka[1]

1.Graduate School of Natural and Technology, Okayama University

An intermediate-depth earthquake (M_{JMA} 6.2) occurred in Iyo-Nada on March 14, 2014. The focal depth is estimated to be 78 km by JMA, and this event occurred in the Philippine Sea slab. In this study, we investigate the early rupture process of the earthquake for three seconds after the initial break. We use P-wave portion on vertical components of waveform records at 50 seismic stations from the seismic networks of JMA, NIED, and AIST. The result of three-dimensional (3D) imaging, we find three strong slip regions S1, S2, and S3 except the hypocenter (S) corresponding to the initial break: S1 is located close to S, northward and upward from the hypocenter at about 0.7 seconds after the initial break, S2 about 9 km southward and 6 km downward at about 2.2 seconds after the initial break, and S3 about 8 km eastward and 7 km downward at about 2.7 seconds after the initial break. From this result, we suggest a fault model with two planes: initial rupture plane including S and S1 with strike of 22°E and dip angle of 69° from JMA's P-wave first motion focal mechanism and the main rupture plane including S2 snd S3 with strike of 244°E and dip angle of 26° from JMA's CMT solution. Then, from the two-dimensional (2D) imaging, we locate the main rupture plane to be 7 km just below the hypocenter. The rupture process is interpreted as follows: a large slip occurred at S1 close to the hypocenter on the initial plane; after the rupture propagated southward and downward on the initial plane and got into the main rupture plane, another large slip occurred at S2; asides, the third large slip then took place at S3.
Acknowledgments: we used the strong motion records of JMA, NIED, and AIST.

Keywords: Initial rupture, Main rupture, Source imaging, 2014 Iyo-Nada intermediate-depth earthquake

What caused the unusual Non-DC component observed in the Jan. 28th 2012 Tanzawa earthquake?

*Shinji Sato[1], Ahyi KIM[1]

1.Yokohama City University

The Tanzawa mountain area is seismically very active: the seismicity in the western Tanzawa is mainly caused by collision of the Izu peninsula and that of the eastern part is caused by subduction of the Phillipine sea plate. Especially in the western part, magnitude (M) ~ 5 earthquake which accompanies similar sized foreshock has been periodically observed. The cause of foreshock is still controversial. The last seismic activity in this region was on Janualy 2012; the M5.4 mainshock occurred on January 28th followed by its M4.7 foreshock occurred 4 minutes later and the aftershock sequence lasted 13 days. One interesting observation of the sequence was that the both foreshock and mainshock exhibited unusual amount of CLVD component whereas similar sized after shock showed nearly pure double couple. The results of the moment tensor inversion using precisely determined hypocenter location and moment rate function analysis indicated that the complex faulting system in the hypocentral area caused the large CLVD. It is consistent with the mechanism differences between ~ M5 earthquakes observed during the sequence. It implies there is a relationship between the complex faulting system and the triggering mechanism of the foreshock.

Keywords: Tanzawa mountain, mechanism, CLVD component, moment tensor inversion, moment rate function

Characteristics of the rupture processes of two large earthquakes off the south-east Kushiro area in Hokkaido in 2004

*Tomoyuki Sagawa[1], Yuichiro Tanioka[1], Takuji Yamada[2]

1.Institute of Seismology and Volcanology, Department of Natural History Sciences,Graduate School of Science,Hokkaido University, 2.Ibaragi University

In this study, Source processes of two Kushiro-oki earthquakes, which occurred in November and December, 2004 (Mw7.1 and Mw6.9), are analyzed. These earthquakes occurred with short time interval and with short distance separation at the same plate boundary. In 1961, two earthquakes of M7 also occurred with a time difference of 3 months at the same plate boundary. In addition, this plate boundary is surrounded by the source area of the large earthquakes of M8, such as the 1973 Nemuro-oki earthquake and the 2003 Tokachi-oki earthquake. Therefore, it is important to study source characteristics of two 2004 Kushiro-oki earthquakes in order to understand the complexity of the plate interface.

We estimate the source time function at each strong motion station (K-net) using empirical green's function method. Then, the directivity effect is analyzed from those estimated source time functions. In consequence, the result suggests that the rupture propagated concentrically for the earthquake occurred in November and propagated about 8 km to the north for the earthquake occurred in December. Moreover, for the earthquake occurred in December, the stress drop was found to be uniform, because few aftershocks occurred within the source area of the earthquake. The earthquake occurred in November affected by the postseismic slip of the Tokachi-oki earthquake. Because the earthquake occurred in December did not increase enough stress at the edge of the source area of the 1973 Nemuro-oki earthquake, the rupture propagated to the north in stead of to the south.

Keywords: 2004 Kushiro-oki earthquake, source process

Dynamic rupture model of the 2014 northern Nagano, central Japan, earthquake (Part 3)

*Yuko Kase[1]

1.Geological Survey of Japan, AIST

We construct a dynamic rupture model of the 2014 northern Nagano, central Japan, earthquake to understand a mechanism of the earthquake and the present condition of the fault. Surface ruptures intermittently observed along the northern part of Kamishiro fault in the southwest of the hypocenter (Katsube et al., 2015). Waveform inversion results, on the other hand, showed that large slip mainly distributed in the northeast of the hypocenter (Asano et al., 2015; Kobayashi et al., 2015; Shiba, 2015; Horikawa, 2015). Kase (2015) constructed dynamic rupture models composed of a single fault or two parallel faults, but could not simulate both the surface rupture distribution and the slip distribution on the fault. In this study, we investigate a fault model with a vertical fault as an initial crack between the two parallel faults, considering the difference between the focal mechanism (JMA, 2014) and the CMT solution (NIED, 2014).
Fault model of the main rupture and tectonic stress field are the same as Kase (2015). Based on the aftershock locations determined by Imanishi and Uchide (2015) and the analysis of the InSAR data (Yarai, 2015), fault strike is N20E, and dip angles of the deeper and shallower regions than 2 km are 60 and 45 degrees. The fault model is composed of two segments: the 10.1 km long northeastern segment corresponding to the large slip region, and the 13 km long southwestern one corresponding to the surface rupture. The fault model has a 2 km left-step with 2 km overlap. In this study, we add a vertical segment with an initial crack between the two main segments. The southern part of the fault reaches the earth's surface, while upper depth of the northern part is 2 km.
Principal stresses are proportional to depth. Azimuth of the maximum principal stress is N60W, and stress ratio is 0.42 (MEXT et al., 2004). The minimum principal stress is vertical, and equal to overburden load. We assume hydrostatic condition. The medium has two-layered structure with 2 km deep boundary, based on the subsurface structure model around the fault (NEID, 2003).
We calculate dynamic rupture processes by the finite-difference method (Kase, 2010), assuming the slip-weakening friction law. The preliminary results show that a rupture initiated on the vertical segment promotes rupture propagation toward the deep portion on the northeastern segment and the shallow portion on the southwestern segment, which agrees with the rupture process of the 2014 northern Nagano earthquake.

Keywords: dynamic rupture, 2014 northern Nagano earthquake, numerical simulation

Relationship between various Source Characteristics and Slip Distribution determined by Source Process Analysis with Teleseismic Body-Wave

*Kenichi Fujita[1], Akio Katsumata[1], Koji Sakoda[2]

1.Meteorological Research Institute, 2.Japan Meteorological Agency

1. Introduction
We have examined optimized preset parameters for automate source process analysis with teleseismic body-wave, and we have become possible to preset optimized parameters based on scaling law without trial and error by analysts.
Then, we compared semi-automatic analysis (automatic analysis except for selecting stations and picking up initial P-wave) with manual analysis, and we confirmed that results were roughly consistent with each other for many events regardless of event magnitude. But, there were differences of slip distribution between semi-automatic analysis and manual analysis for some events.
We examine source characteristics which would reflect differences of slip distribution by comparing with aftershock distribution, tsunami source area, etc.

2. Analysis Methods
We used the same program package as Iwakiri et al. (2014) for analyzing source process with teleseismic body-wave. We used broadband waveform data which were downloaded from IRIS DMC HP, and set sampling time and band-pass filter depending on event magnitude. We used epicenter data of JMA for events in and around Japan, and USGS for events in other areas. We used focal mechanism data of JMA for events in and around Japan, and GCMT or others for events in other areas. Hypocenter was set at center of assumed fault plane, and subfaults size and number were set depending on event magnitude. Source-time function were set with triangle functions, and number of basis function and rise time were set depending on event magnitude. Analysis time was set at sum of time necessary for rupture front arriving at most distant subfault (from hypocenter) and time destruction allowed at subfault. Velocity structure for Green's functions were set based on the IASP91 model, and the CRUST2.0 model for near hypocenter. We used the ABIC (Akaike (1980)) for temporal and spatial smoothing constraints, and set hyperparameters as ABIC value become minimum. Maximum rupture speed was set at 0.72 times of S-wave velocity from empirical relationship of Geller (1976).

3. Comparing Methods
(1) We investigated number of aftershock on subfaults, and compared with slippage.
(2) We calculated crustal deformation of land or seafloor surface from slip distribution, and compared with tsunami source area.
(3) We investigated location of the maximum aftershock and slip distribution of the maximum aftershock, and compared with slippage.

Keywords: Source Process Analysis, Slip Distribution

Simulation of Recurring Earthquakes along the Japan Trench

*Kenichi Fujita[1], Fuyuki Hirose[1], Kenji Maeda[1]

1.Meteorological Research Institute

1. Introduction

Magnitude (M) 7-8 earthquakes have been known to occur repeatedly along the Japan Trench by historical evidences. Recently the occurrence of the 2011 off the Pacific coast of Tohoku earthquake has proved the possibility of recurrence of M9 class earthquakes.

Basing on these data of the past earthquakes, we try to make the numerical simulation model reproducing magnitude (about 7-9) and recurrence interval (T) estimated for earthquakes recurring along the Japan Trench.

2. Methods

The target earthquakes that are known to occur repeatedly and we aim to simulated are the northern Sanriku earthquake (M~8.0, T~100 years), the Miyagi-oki earthquake (M~7.5, T~40 years), the near trench southern Sanriku earthquake (M~8.0, T~110 years), the Ibaraki-oki earthquake (M~7.0, T~20 years), and the type of The 2011 off the Pacific coast of Tohoku earthquake (M~9.0, T~600 years). In addition, we tried to reproduce the characteristics of earthquakes near trench northern Sanriku (1896 Meiji-Sanriku earthquake of Mt~8.6-9.0) and around Fukushima-oki (1938 Fukushima-oki earthquake swarm of M~7.4) whose repeatability, however, is not clear.

We used the equation of motion considering shear-stress reduction (Rice (1993)), and adopted the composite law (Kato and Tullis (2001)) for the rate- and state-dependent friction law. Analysis region was set largely enough to surround all asperities of the target earthquakes. We used the three-dimensional plate configuration of Nakajima and Hasegawa (2006), and set 17,507 triangular cells of the seize about 5 km. Subducting rate of the Pacific plate against land plate was put 8.0-8.2 cm/year from south to north referring to Wei and Seno (1998) etc. Frictional parameters (a, b, L) were chosen to reproduce magnitude and recurrence interval of the earthquakes by trial and error. We basically consider two types of parameter sets: Case 1 (background stable slip model), region surrounding asperities (background) is velocity strengthening ($a-b > 0$), Case 2 (hierarchical model), background is velocity weakening ($a-b < 0$).

3. Results

Magnitude and recurrence interval of earthquakes we simulated in our model as follows. In the case 1, the northern Sanriku earthquakes are (M~8.0, T~61-103 years), the Miyagi-oki earthquakes (M~7.4, T~30-74 years), the near trench southern Sanriku earthquakes (M~7.9, T~104-130 years), the Ibaraki-oki earthquakes (M~6.8, T~14-52 years), and the type of The 2011 off the Pacific coast of Tohoku Earthquake (M~8.3, T~203-232 years (the latter half magnitude of M8 class earthquakes occurred once every few times). It is noteworthy that near trench northern Sanriku earthquakes occurred a few years after the northern Sanriku earthquakes, and swarm-like Fukushima-oki earthquakes occurred in some cases.

In the case 2, the northern Sanriku earthquakes (M~7.9, T~66-140 years), the Miyagi-oki earthquakes (M~7.3, T~31-149 years), the near trench southern Sanriku earthquakes (M~7.8, T~120-216 years), and Ibaraki-oki earthquakes (M~6.8, T~9-51 years), and the type of the 2011 off the Pacific coast of Tohoku earthquake (M~8.5, T~294-526 years (M9 earthquakes occurred once every few times). In this case, near trench northern Sanriku earthquakes didn't occur, but swarm-like Fukushima-oki earthquakes occurred in some cases.

In the future studies, we will examine frictional parameters further in order to make more realistic numerical simulation models.

Keywords: Simulation of Recurring Earthquakes, The 2011 off the Pacific coast of Tohoku Earthquake

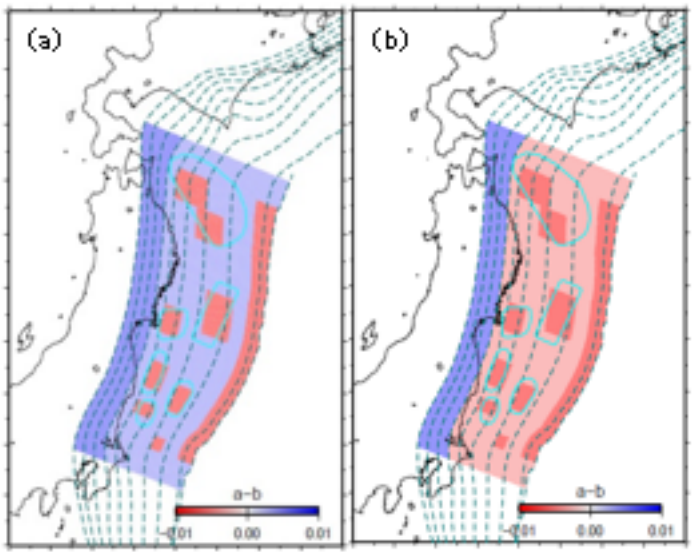

Figure 1. Friction parameter (a - b) (a) background stable slip model (b) hierarchical model

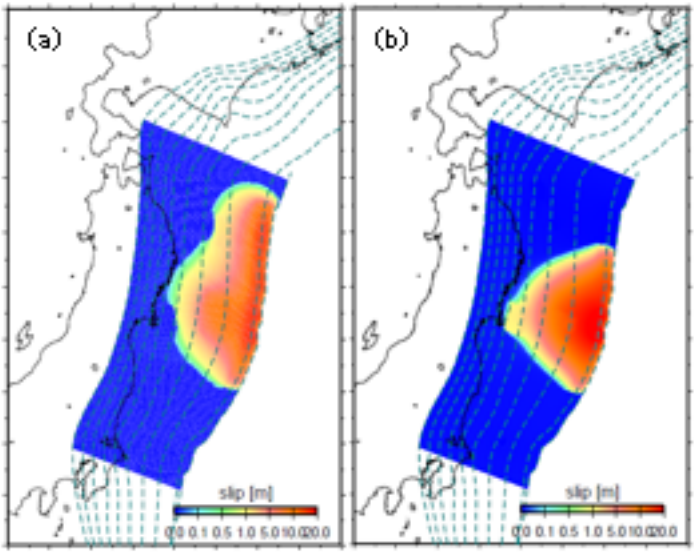

Figure 2. Slip distribution (a) background stable slip model (b) hierarchical model

Simulation of the Nankai earthquake cycle -Quasi-dynamic discrete-cell model incorporating rate-weakening due to thermal pressurization-

*Yugo Ozaki[1], Kazuro Hirahara[1]

1.Graduate School of Science, Kyoto University

Along the Nankai Tough, great earthquakes have historically recurred, causing devastating disasters in southwest Japan, and the next Nankai earthquake is anticipated to occur in the first half of this century. The recurrence times of the Nankai earthquakes vary from 90 to 250 years. The source region extending from off-Shikoku to off-Tokai regions is divided into five segments. The segments complicatedly slip at each event; all five segments seismically slip, and some segments seismically slip with delays or sometimes not slip (Ishibashi, 2004). Moreover Seno [2012] re-examined the historical sequences and proposed that the source region is characterized into a seismic-b, tsunami-b and geodetic-b areas where seismic waves, tsunamis and crustal deformations are dominantly generated, respectively, and the historical events are grouped into the Ansei-type or the Hoei-type. His model might explain the complexity of historical sequences, but we need some verification. We execute earthquake cycle simulations to reveal the complexity.
In this study, we take a boundary element method to simulate earthquake cycles following the rate- and state-dependent friction law. Setting spatially heterogeneous friction parameters on the fault may not reproduce the complex historical sequences, and another factor should be introduced in the numerical model. Noda and Lapusta [2010] focused on the thermal pressurization (TP) that the increases pore fluid pressure at the shear zone due to frictional heating and showed that the interaction of two patches with spatially heterogeneous hydraulic parameters produces complex earthquakes cycles. The goal of this study is to reproduce the complex sequences by introducing TP in addition to spatially heterogeneous frictional parameters in the model. Their simulation include the dynamic rupture process, but in this study we use the radiation damping (Rice,1993) to simulate quasi-dynamically for reducing the computational cost. The quasi-dynamic approximation may cause the underestimation of TP effect, which should be examined in future.
TP increases the effective normal stress, and then the friction drops coseismically. Therefore the amount of coseismic slip increases and the recurrence interval gets longer than that without TP. For calculating the temporal change in pore fluid pressure by TP, we use the convolution form proposed by Bizzari and Cocco [2012] which enables us to take a longer time step than that in the case solving numerically the diffusion equation. However, the numerical cost of convolution calculation is also enormous. Accordingly, it is quite difficult to execute cycles of great earthquakes such as Nankai earthquakes as in a continuum medium, considering also the numerical cost of calculating interaction between a huge number of cells. Hence we consider a conceptual model similar to the block and spring model [Mitsui and Hirahara, 2004]. The numerical cost using their model is relatively smaller even when taking account of thermal pressurization. They set five blocks corresponding to five segments and assign properties to respective blocks; for example, dip angles, plate convergence rates and frictional parameters. In this study we calculate slip response functions by the code of Okada [1992] for elastic interactions between cells instead of springs, which is called a discrete cell model. Because we found only five cells produce almost no interactions, we divide each cell to a number of cells along its subduction direction. In addition to a variety of frictional parameter settings, we apply TP to specific cells and we compare the calculated patterns of earthquake cycle with the historical sequences of the Nankai earthquakes. This conceptual model and the resultant earthquake cyclers are expected to contribute to the actual reproduction of the Nankai earthquake sequences by simulating not as a discrete cell model but as a

continuum model.

Keywords: Nankai Trough, simulation of earthquake cycle, a boundary elementary method, pore fluid pressure, thermal pressurization

Simulated precursory large aseismic slip at the deeper extension of the seismic region along the Nankai Trough, SW Japan

*Makiko Ohtani[1], Nobuki Kame[1], Masao Nakatani[1]

1.Earthquake Research Institute, The University of Tokyo

At the subduction zone along the Nankai Trough, SW Japan, large earthquakes around M8 had occurred repeatedly. Their intervals (around 100–200 years) have been identified precisely from old historical documents combined with geological surveys (*Sangawa*, 2011). The most recent events occurred in 1944 (the Showa To-Nankai EQ.) and 1946 (the Showa Nankai EQ.) when modern satellite geodetic networks had not been developed yet.
The existence of short-term aseismic processes before the 1944 and 1946 events has been inferred from the leveling or interview records. Two-times level difference measurements showed the displacement of north down before the 1944 event (*Mogi*, 1986), and the water level of some wells were reported to have dropped before the 1946 event (*Sato*, 1982). These phenomena were observed within several days before the earthquakes, and each could have been caused by 2 m slip on the plate interface at the deeper extension of the seismic region before each event (*Linde and Sacks*, 2002).
In this study, we simulate the cycle of large earthquakes in a quasi-dynamic 2D model to investigate aseismic slip acceleration in the deeper extension of seismic fault. We consider a flat plate interface with a shallow dipping angle of 15° for the depth 0–60 km mimicking the Nankai Trough. Following *Nakatani and Scholz* (2006) and *Yoshida et al.* (2013), we introduce an intrinsic cut-off time for healing into the state evolution law of the rate-and-state friction. The intrinsic time leads to a corresponding cut-off velocity (V_{cx}) beyond which velocity strengthening occurs. We assume that V_{cx} is depth dependent (1–10^{-9} m/s). We show that this depth variation in V_{cx} can possibly produce large aseismic slip.
In our simulation, the bottom part of the fault below the deeper extension exhibits a constant slip rate loaded by a subducting plate velocity (4.5 cm/year). This bottom slip drives the adjacent deeper locked part and aseismic slip starts to accelerate. Because of the introduction of low V_{cx} there, the slip cannot monotonously accelerate to seismic slip at the same depth. Instead, the aseismic slip propagates to the shallower part where the slip accelerates following the increasingly higher V_{cx} at the depth, and finally reaches to seismic slip at the shallow part with the large V_{cx}. The seismic slip starting at shallow part then propagates bilaterally to the shallower and deeper parts, and develops into a large earthquake. For example, the point at 20 km depth starts to slip aseismically 5.4 days before the earthquake and 54% of the slip occurs as the precursory aseismic slip. The deeper part produces the longer-lasting aseismic slip with the smaller velocity.
This simulated aseismic slip may correspond to the several-days precursors of the 1944/1946 events. Our results also suggest that the observed short-term aseismic slip acceleration is a part of the longer-term aseismic slip that has started at deeper parts, which may be detected at the next To-nankai/Nankai earthquakes with the help of recently installed modern observation networks (Do-Net, Hi-Net, and GEONET) around the Nankai region.
This study was supported by the Ministry of Education, Culture, Sports, Science and Technology (MEXT) of Japan, under its Earthquake and Volcano Hazards Observation and Research Program.

Keywords: Nankai Trough, precursory slip, cycle simulation

Numerical simulation of slow slip events, considering the effect of earth tide

*Takanori Matsuzawa[1], Yoshiyuki Tanaka[2], Bunichiro Shibazaki[3]

1.National Research Institute for Earth Science and Disaster Prevention, 2.Earthquake Research Institute, the University of Tokyo, 3.Building Reserach Institute

Several studies reported that occurrence of slow slip events (SSEs) in the Nankai region is affected by earth tide (e.g., Nakata et al., 2008; Tanaka and Ide, 2014). The effect on the SSEs is also examined by numerical studies (e.g., Hawthorne and Rubin, 2013). We have studied the behavior of SSEs during seismic cycles in numerical simulations (e.g., Matsuzawa et al., 2010), and suggested that recurrence intervals may decrease at the later stage in a seismic cycle. In this study, we examined the behavior of SSEs during seismic cycles, considering the effect of earth tide.
Our numerical model is similar to our previous study with a flat plate interface (i.e., Matsuzawa et al., 2010). A plate interface is expressed by 40,000 small rectangular elements. A rate- and state-dependent friction law with a cutoff velocity is adopted as the friction law on each element. In the region deeper than short-term SSEs, low cutoff velocity ($10^{-6.5}$ m/s) and low effective normal stress are assumed. In the following section, we show an example in the case of sinusoidal stress perturbation at the period of M2 tide (i.e. 12.42 hours) with 2 kPa peak-to-peak amplitude, which has the phase that maximum shear stress coincides with minimum normal stress.
In the numerical result, introduction of earth tide slightly decreases recurrence interval of megathrust earthquakes, for example, from 106.5 years to 106.2 years between first and second large earthquakes, and from 106.5 years to 105.9 years between second and third large earthquakes. This suggests that the earth tide can also affect the recurrence intervals of large earthquakes.
In terms of short-term SSEs, the recurrence intervals decrease during a seismic cycle both in the cases with and without tidal effect. The difference between these two cases is not clear. We note that SSEs are detected on each rectangular element, if displacement exceeds 5 mm during episodic slip with more than twice of subduction velocity. In terms of the relationships between the occurrence of SSEs and phase of tides, the distribution of occurrence times of SSEs shows a peak around the phase with maximum shear stress and minimum normal stress. The SSEs, which occur between -30 and 30 degrees from this phase, are 22.7%, 22.7%, and 22.2% of the total number of SSEs, during the period of 5-35 years, 35-65 years, and 65-95 years after large earthquakes, respectively. These values are higher than the identical ratio of 16.7% with no relevance. Our numerical simulation also suggests that the stress perturbation by earth tide can affect the occurrence of SSEs, although the change during seismic cycle is not clear in this case.

Keywords: Slow slip event, Numerical simulation, Earth tide

Dependencies of pore pressure and fracture distribution on elastic wave velocities for thermally cracked rocks : Implications for high Vp/Vs zone related to slow slip events along plate boundary

Kaya Nishimura[1], *Shinichi Uehara[2], Kazuo Mizoguchi[3], Kohei Seto[2], Kenji Kawashima[2]

1.Graduate School of Science, Toho University, 2.Faculty of Science, Toho University, 3.Central Research Institute of Electric Power Industry

Seismic studies have found that there are high Vp/Vs ratio regions in oceanic crusts at subducting oceanic plates (e.g., Cascadia (2.0-2.8) (Audet et al., 2009), Nankai trough (> 2.03) (Kodaira et al., 2004)), and the correlations between the location of high Vp/Vs and slow slip zone have been pointed out by several studies. Christensen (1984) indicated that high pore pressure may cause high Vp/Vs. It is also known that Vp/Vs also depends on porosity or pore structures (fracture distributions). However, the relationships between Vp/Vs, pore pressure, porosity and fracture distribution have no investigated in detail for rocks composing oceanic crusts.
This study reports the results of measurements of Vp and Vs (transmission method) at controlled confining and pore pressure and estimation of Vp/Vs ratio for thermally cracked dolerite and relation between Vp/Vs, pore pressure and fracture distributions. Confining pressure was constant (50 MPa) and pore pressure was decreased from 49 to 0.1 MPa and then increased to 49 MPa. We did measurement with an intact rock specimen (0.5% in porosity) and the rock specimens heated under 300, 500 and 700°C for 24 hours (2.1%, 3.4% and 3.5% in porosity, respectively). Rock specimens heated under 500 and 700°C were reddish in color, which suggested a possibility that not only cracking but also oxidizations of rock forming minerals might affect elastic velocities. Therefore, we operated elastic velocity measurements under atmospheric pressure with rock specimens heated under 500 and 700°C at air (an oxygen concentration is around 21%) and at nitrogen conditions (an oxygen concentration is less than 0.5%), and revealed that the effect of oxidization on Vp/Vs is several times less than the effect of heating-temperature conditions.
In this experiments, for the intact rock specimen and specimen heated under 300°C, Vp and Vs was almost constant at any pore pressure, and for specimen heated under 300°C, Vp/Vs was 1.7 to 1.8, which is less than the high Vp/Vs ratio observed at oceanic crusts of subducting plates. On the other hand, for specimens thermally cracked under 500 and 700°C, Vp/Vs increased as pore pressure was increased (effective pressure was decreased), and was more than 2 when pore pressure was over 40 MPa and 30 MPa, respectively. This results indicate that Vp/Vs is not over 2 unless porosity is larger enough (approximately 3% for the results in this study), even if pore pressure is higher.
We also observed fractures in the specimens by using a microscope, and measured fracture densities. The fracture densities for the specimens heated under 500 and 700°C were larger than that of the intact rock specimen. There was no clear difference on the fracture density between the specimens heated under 500 and 700°C, but microscope observations revealed that there was differences on fracture distributions such that fine net-like fracture distributions or networks of intra-mineral fractures were observed more for the specimen heated under 700°C than that under 500°C. These features on fracture distributions might affect elastic velocities. In general, high Vp/Vs near slow slip zones tends to be simply interpreted as high pore pressure, but it may also be influenced by porosity and features of fracture distributions.
This work was supported by JSPS Grant-in-Aid for Scientific Research (Grant Number 26400492) .

Keywords: high Vp/Vs, laboratory experiment, fracture density, high pore pressure

Effect of fault surface evolution on slow slip behaviors in large-scale biaxial experiments

*Futoshi Yamashita[1], Eiichi Fukuyama[1], Shiqing Xu[1], Kazuo Mizoguchi[2], Shigeru Takizawa[1], Hironori Kawakata[3]

1.National Research Institute for Earth Science and Disaster Prevention, 2.Central Research Institute of Electric Power Industry, 3.Ritsumeikan University

To investigate the preparation process preceding the main fast rupture under more realistic condition, we conducted stick-slip experiments using large-scale biaxial friction apparatus at NIED in Tsukuba, Japan. We used two rectangular metagabbro blocks as specimen, whose contacting area was 1.5 m long and 0.1 m wide. The experiments were repeatedly conducted with same pair of specimens, which means the fault surface evolved with the frictional slip. We successively conducted a set of three experiments under the condition of constant normal stress of 6.7 MPa and loading rate of 0.01 mm/s. All wear materials were collected after each experiment. To artificially accelerate fault evolution from one stage to the next, we applied fast loading with long slip displacement between a set of three experiments. As a result, we obtained three sets of the experimental result in different evolutional stages I, II and III; one and two fast-loading processes mentioned above were performed before the experimental sets in Stage II and III, respectively. In all experiments, we observed many stick-slip events, the number of which tended to increase with the maturity of the fault. Local strain array also showed slow propagation of shear stress drop, which was derived from slow slip before the main rupture. We found that the occurrence location of slow slip and its occurrence time relative to the main rupture, depend on the stage of fault evolution. In Stage I, both the temporal and spatial distributions of the slow slip occurrence were mono-modal, whereas a variety of occurrence times were observed in Stage II and III. The occurrence locations in Stage I and II look consistent with the initial normal pressure distribution on the fault, which was estimated from pressure sheet measurements (Fujifilm PRESCALE LW) just before each experiment; slow slips started to propagate from the location where the initial normal pressure is at a local minimum. On the contrary, we cannot find such clear relationship in Stage III, though some of the occurrence locations look related to the distribution of wear material generated with the frictional slip. These results suggest that the fault surface evolution may increase the complexity of slow slip behaviors.

Keywords: Slow slip, Fault evolution, Friction experiment

Transient Frictional Behavior Observed in the Velocity-Stepping Test of Gabbro Conducted at Intermediate to High Slip Velocities

*Ryuji Nakano[1], Akito Tsutsumi[1]

1.Graduate School of Science, Kyoto University

Since Brace and Byerlee [1966] suggested that frictional stick-slip sliding plays an important role in seismic faulting, a number of friction experiments have been carried out. One of the greatest achievements is a proposal of rate- and state-dependent friction constitutive law by Dieterich [1978]. This law has been widely used for simulating earthquake cycles, but the law was originally proposed at low slip velocities of the order of sub-mms^{-1}, and it has not been clarified whether rate- and state-dependent friction constitutive law can be applied to frictional phenomena at seismic faulting slip velocities (the order of ms^{-1}).
In this study, we modified a rotary-shear friction apparatus at Kyoto University and performed a series of intermediate to high slip velocity friction experiment with velocity stepping by using this apparatus. In this experiment, we used a pair of hollow cylindrical gabbro blocks with an inner-diameter of 26 mm and an outer-diameter of 40 mm, and changed the rotation rate of the servomotor in this apparatus from one value to another; hereinafter we call the former value *IRPM* and the difference value between the former and the latter *ΔRPM*, respectively. We selected all the combinations of IRPM and ΔRPM throughout this experiment: a value of IRPM of either 10, 20, 50 or 100 RPM, and a value of ΔRPM of either 30, 80, 150, 200, 300 or 400 RPM. This experiment was carried out under a constant normal stress of 1.5 MPa.
The friction response to the imposed slip velocity steps is characterized by two strength peaks and slip-weakening phases that follow each of the peaks. Typical behavior of the transient was observed in the tests conducted at an IRPM value of 20 RPM and a ΔRPM value of 200 RPM. Rotation rate overshoots the target value once and is converged to the value while oscillating because of high value of the speed loop gain integration time constant of the servomotor in this apparatus during this experiment. Considering this servomotor behavior, the first strength peak is reached while the rotation rate is accelerating, and the second peak is reached when the rotation rate reaches its peak value. Interestingly to note, the transient behavior of friction response recorded in this study is similar to those observed in friction melting experiments [e.g., Hirose and Shimamoto, 2005]. There are many kinds of friction constitutive law, but existing friction constitutive laws may not describe this behavior. A constitutive model for frictional sliding that is capable of describing the transient behavior observed at intermediate to high slip velocity tests in this study is required to be developed.

Keywords: Friction experiment, Friction constitutive law, Intermediate to high slip velocity

Frictional properties of pre- and post-subducting oceanic basement rocks

Ken Kohama[1], *Yujin Kitamura[2], Akito Tsutsumi[3]

1.Department of Earth and Environmental Sciences, Faculty of Science, Kagoshima University, 2.Department of Earth and Environmental Sciences, Graduate School of Science and Engineering, Kagoshima University, 3.Graduate School of Science, Kyoto University

On the faults in the subduction plate boundary, fault slips when the shear stress exceeds the strength of the rock interface between the hanging and footwall. Seismic slip is associated when the frictional strength decreases with the slip. The up-dip limit of the seismogenic zone coincides with the stepping down of the décollement to the oceanic basement. Seismogenic process is thought to undergo in the upper part of the oceanic crust (Kimura and Ludden, 1995; Bangs et al., 2009). Tectonic mélanges of the Shimanto belt which is formed along the plate boundary fault zone (Kitamura et al., 2005) contains basalts with cataclastic shear zones. To understand the seismogenic process, therefore, basalts are key material and it is essential to know their frictional properties. Here we performed frictional experiment on the basalts from pre-subduction drilled core in the Nankai trough and post-subduction outcrop in the Shimanto belt.
We performed friction experiments using the rotary shear, an intermediate to high velocity frictional testing apparatus in Kyoto University. Basalt samples were taken from IODP Expedition 333 Site C0012 as pre-subduction materials (C12G8R, C12G10R) and from the Mugi tectonic mèlange as postsubduction material (MBN-3). We performed constant low velocity test with normal stress of 2 MPa and rotational speed of 0.012 r.p.m with all three samples, and velocity stepping test to evaluate the velocity dependence with two samples (C12G8R, MBN-3) with normal stresses of 2 MPa and 5 MPa.
Results of the constant low velocity test showed the steady frictional coefficient of C12G8R, C12G10R and MBN-3 ranging from 0.70 to 0.84 (average 0.76), from 0.60 to 0.79 (ave. 0.67) and from 0.50 to 0.63 (ave. 0.57), respectively. On the velocity stepping tests, C12G8R and MBN-3 with normal stress of 2 MPa showed neutral depencence of the friction coefficient to the velocity. But, C12G8R with normal stress of 5 MPa showed velocity strengthening behavior and MBN-3 with normal stress of 5 MPa showed velocity weakening behavior.
The constant low velocity tests revealed that the frictional coefficient of MBN-3 is lower than those of C12G8R/C12G10R. This implies that the post-subduction basalt is essentially weaker. From the results of velocity stepping tests, pre-subducting basalt (C12G8R) without preexisting gouge on the interface (5 MPa, menu 1) showed notable velocity strengthening. Other runs at 5 MPa are velocity neutral or strengthening. On the other hand, post subducting basalt (MBN-3) showed velocity weakening at 5 MPa, menu 1 and 2. These results suggest that the subducting oceanic crust progressively changes its frictional property that enables the rocks to be potent in seismogenesis may leading to the stepping down of the decollement to the oceanic basement at the up-dip limit of seismogenic zone.

Reference

BANGS, N. L. B., et al. Broad, weak regions of the Nankai Megathrust and implications for shallow coseismic slip. *Earth and Planetary Science Letters*, 2009, 284.1: 44-49.
KIMURA, Gaku; LUDDEN, John. Peeling oceanic crust in subduction zones. *Geology*, 1995, 23.3: 217-220.
KITAMURA, Yujin, et al. Mélange and its seismogenic roof décollement: a plate boundary fault rock in the subduction zone—an example from the Shimanto Belt, Japan. *Tectonics*, 2005, 24.5.

Keywords: Nankai Trough, Shimanto Belt, Frictional experiment, basalt, velocity weakening

Evolution of fault surface state during frictional weakening of quartz rocks

*Hirotaka Iida[1], Akito Tsutsumi[1]

1. Graduate School of Science, Kyoto University

Siliceous rocks such as novaculite and quartzite display dramatic weakening of frictional strength at slip velocities of >1 mm/s [Goldsby and Tullis, 2002; and Di Toro et al., 2004].It has been suggested that the frictional weakening likely resulted from production and shearing of hydrated amorphous silica layer along a fault in quartz rocks. However, there exists little information on the frictionally-generated material; consequently the mechanism of the weakening remains poorly understood. In this study, to better characterize the state evolution of the fault surfaces of quartz rocks during the slip-weakening, we have performed SEM and stereo microscope observation of the fault surface and XRD analysis of the gouge formed on the fault.
All the experiments in this study were conducted using a rotary-shear, intermediate-to high-velocity friction testing machine in Kyoto University. The test samples used for the friction experiments were chert from the Tamba Belt, northern Kyoto prefecture, Japan, which is a Jurassic accretionary complex, and single crystal of quartz (a synthetic crystal). A pair of solid cylinders with a ring-shaped end surface (inner and outer diameter of 5 mm and 25 mm) was cored from the samples. Experiments were carried out under a constant normal stress condition of 1.5 MPa and at slip velocities of 105 mm/s, 10.5 mm/s and 1.05 mm/s.
Experimental results reveal that slip-weakening occurs at all the tested slip velocity conditions. At slip velocity of 105mm/s, both of the quartz and the chert specimens show very low friction coefficient value of 0.1 to 0.2 after the slip-weakening. The values of the slip-weakening distance (D_c) of this study are 0.2 to 0.3 m for the quartz specimens and 0.7 to 1.5 m for the chert specimens, respectively. These values are by an order of magnitude smaller than the D_c value reported in Hayashi and Tsutsumi [2010]. The D_c value appears to depend on the parallelism of the initial fault surfaces.
Fault surfaces after the experiments are covered by white, fine-grained gouge. The SEM observation reveals the development of asymmetric flake-like structure on the sliding surface, which is characterized by tearing of the surface material with approximate size of 100 to 300 μm. The XRD analyses reveal that only the chert specimen that had slipped for large displacement after the slip-weakening behavior contains amorphous material. This result suggests that the gouge material formed during the slip-weakening period is not amorphous.

Foreshock activity during stick-slip experiments of large rock samples

*Yushi Tsujimura[1], Hironori Kawakata[1], Eiichi Fukuyama[2], Futoshi Yamashita[2], Shiqing Xu[2], Kazuo Mizoguchi[2,3], Shigeru Takizawa[2], Shiro Hirano[1]

1.Ritsumeikan University, 2.NIED, 3.CRIEPI

For inland earthquakes such as the 2007 Noto Hanto earthquake (Doi and Kawakata, 2013) and the 2008 Iwate-Miyagi earthquake (Doi and Kawakata, 2012), foreshocks were reported to occur in the vicinity of main shock hypocenter. Moreover, for interplate earthquakes such as the 2011 off the Pacific coast of Tohoku earthquake (Kato, et al., 2012) and 2014 Iquique earthquake in Chile (Yagi et al., 2014), migration of foreshocks toward the main shock hypocenter was detected in one month before the main shock. In order to understand the generation mechanism of foreshocks, it is important to investigate under what environments foreshocks occur.
Since 2012, stick-slip experiments have been carried out using a large-scale biaxial friction apparatus at NIED (e.g., Fukuyama et al., 2014). Based on the experimental result that foreshocks were detected only in the later period of each run, Kawakata et al. (2014) suggested that the foreshocks occur only after the generation of gouge. In this study, we carried out a series of stick-slip experiments with and without pre-existing gouge along a fault plane to confirm if fault gouge affects the foreshock activity. When foreshocks are detected, we estimate the hypocenter locations of foreshocks.
We used two rectangular metagabbro blocks to make the simulated fault plane, whose dimension was 1500 mm long and 500 mm wide. The experiments were conducted under normal stress of 1.33 MPa and loading speed of 0.01 mm/s up to approximate slip amount of 8 mm. During each experiment, we continuously measured elastic waves to detect foreshocks. The sensor distribution is shown in the figure below. Gouge materials were prepared naturally during preceding experiments whose sliding speed was as high as 1 mm/s.
To roughly detect foreshock activity, we calculated cumulative amplitude of continuous waveform data every 0.01 seconds. During an experiment without pre-existing gouge materials (LB13-004), a few foreshocks were detected. On the other hand, during an experiment with pre-existing gouge materials (LB13-007), much more foreshocks were detected. Then we estimated hypocenters of foreshocks for a stick-slip event (event 44) in LB13-007. Although the initial phases of the main shock were contaminated due to the coda wave signals of preceding foreshocks, the hypocenter of the main shock was roughly estimated near the right end of the fault plane. Foreshocks began to occur in the left half of the fault plane, but most of later foreshocks occurred near the right end. Therefore, we confirmed that foreshock activity was high when gouge materials were present along a fault plane, and found a similar hypocenter migration of foreshocks toward the main shock hypocenter, which was reported for interplate earthquakes.
In the future, we shall examine the data obtained from other experiments to confirm if the aforementioned features are common.
Acknowledgments: This work was supported by NIED research project “Development of monitoring and forecasting technology for crustal activity” and JSPS KAKENHI Grant Number 23340131.

Keywords: large-scale biaxial experiments, foreshock activity, fault gouge

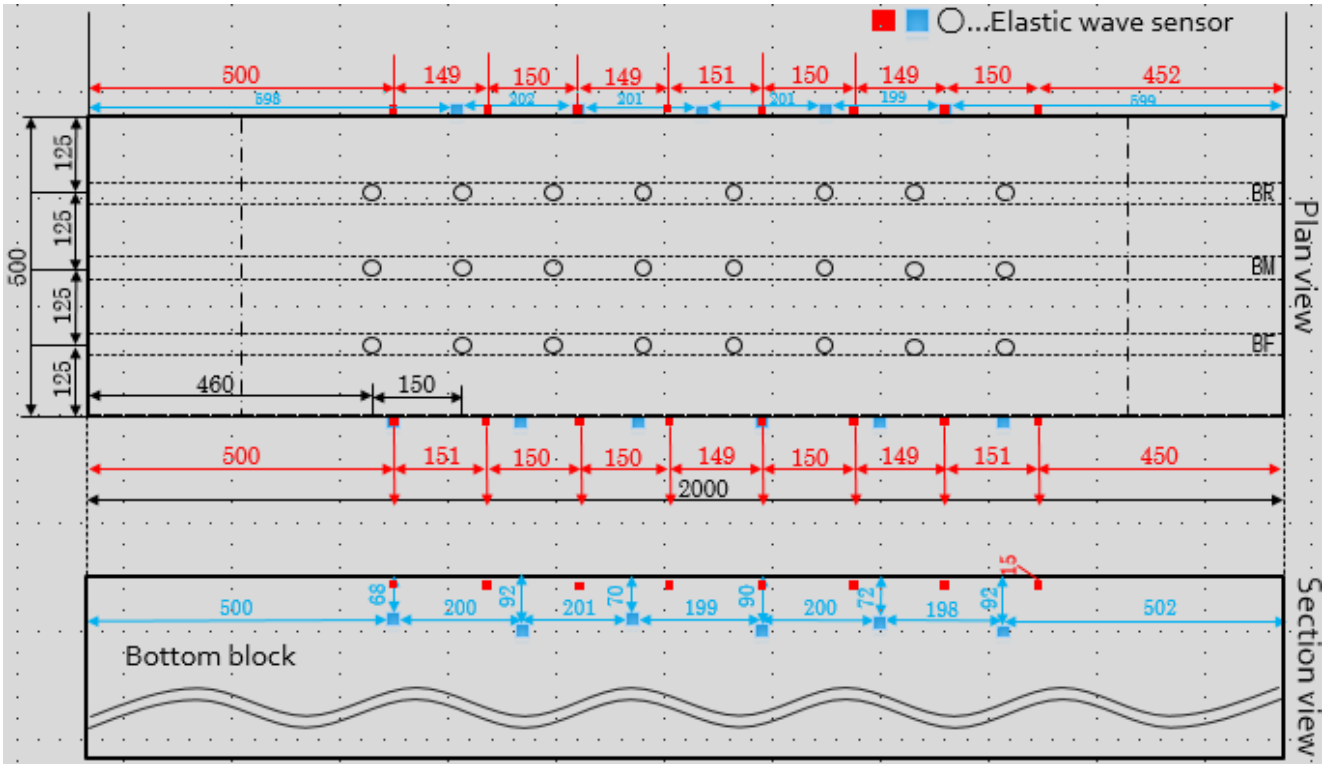

Frictional behavior of smectite-bearing fault gouges in large displacement frictional experiments under constant pore pressure

Tomoaki Kawai[1], *Akito Tsutsumi[1]

1.Graduate School of Science, Kyoto University

Frictional properties of smectite-bearing material at large displacements should provide valuable information for the stability of slip in the shallow parts of subduction zone faults. However, most of the previous experiments are limited by the amount of displacement that can be achieved and the frictional behavior at large displacements remains poorly understood. In this study, we have conducted large displacement friction experiments on mixtures of montmorillonite and quartz at constant pore pressure. Our purpose of this study is to investigate the correlations between gouge textures and frictional velocity dependence of smectite-bearing faults.
We examined frictional behavior and internal textures of simulated gouge samples composed of montmorillonite/quartz mixtures. Two different compositions of the gouges were tested: mixtures of montmorillonite/quartz = 20/80 (abbreviated as Mnt20/Qtz80) and 40/60 wt% (Mnt40/Qtz60), respectively. We sheared the gouges in rotary shear to displacements of more than 1 m at a normal stress of 10 MPa and at a constant pore pressure of 5 MPa. During the shearing, these gouges were subjected to velocity step changes to examine the velocity dependence of friction for a range of slip velocities v from 0.003 to 0.3 mm/s.
Results of the experiments reveal influences of the composition, displacements and slip velocities on the frictional behavior. Both Mnt20/Qtz80 and Mnt40/Qtz60 gouges show slip-hardening behavior. Positive friction velocity dependence was observed in both gouges at short displacement for all the tested slip velocities. At large displacement (v > 30 mm), Mnt20/Qtz80 gouge shows negative friction velocity dependence for all the tested slip velocities. On the contrary, friction of Mnt40/Qtz60 gouge exhibits negative velocity dependence for lower velocities (0.003 mm/s to 0.03 mm/s) and positive velocity dependence for higher velocity stepping (0.03 mm/s to 0.3 mm/s). The SEM observation of the Mnt20/Qtz80 gouge reveals that montmorillonite particles are agglomerated initially to form montmorillonite-filled matrix domains. With continued displacement, the agglomerated distribution of montmorillonite becomes to be disaggregated; eventually the montmorillonite particles are incorporated into the fine-grained matrix of the gouge. Grain size of quartz decreases with displacement, during which change the grain shape of the quartz becomes to be more rounded. It appears that increasing degree of size reduction of quartz grains and a more scatter distribution of montmorillonite particles correlate with a more negative velocity dependence of friction.

Keywords: velocity dependence of friction, montmorillonite, large displacements

Experimental demonstration for blackening of pseudotachylyte

*Yuki Nakano[1], Shunya Kaneki[1], Tetsuro Hirono[1]

1.Department of Earth and Space Science, Graduate School of Science Osaka University

Pseudotachylyte, basically formed by frictional melting at earthquake, sometimes shows various colors of not only black but also of greenish black and grayish black. The color might be correlated to the mineral assemblage, slip parameter, and environmental condition, but such relationship has not yet been investigated. We here demonstrated to form pseudotachylyte by using high-temperature furnace on the artificial mixture samples of quartz, albite, biotite, and chlorite. The melted product after heating the mixture of quartz and albite at 1300 °C did not show the blackening, whereas the products using the mixtures with 10 wt.% biotite and/or 10 wt.% chlorite became remarkably black. By taking consideration into the SEM-ESD data, we concluded that Fe-bearing minerals plays an important role for the color transition, especially, blackening in pseudotachylyte.

Keywords: pseudotachylyte, blackening

Formation of pseudotachylyte in the lower crust plastic regimes: Evidence from the Woodroffe thrust, central Australi

*Takako Satsukawa[1], Aiming Lin[1]

1.Department of Geophysics, Division of Earth and Planetary Sciences, Kyoto University

Most reported fault-related pseudotachylytes are cataclasite-related, which have formed at shallow depths in brittle dominated seismogenic fault zones by both frictional melting and crushing mechanisms. Pseudotachylyte has also been described in association with mylonitic rocks having formed in deep-level fault shear zones within the semi-brittle to crystal-plastic regimes. However, the mechanism of coseismic shear zone formation in the lower crust is still poorly understood.
A >3.0 km-wide pseudotachylyte generation zone including a 1.5 km-wide mylonitized shear zone marked by large volumes of sub-mm- to cm-scale pseudotachylyte veins is developed along the Woodroffe thrust (central Australia) (Lin et al., 2005; Lin, 2008). The pseudotachylytes display typical melt-origin features, including rounded and embayed clasts, spherulitic and dendritic microlites, and flow structures within a fine-grained matrix. Three types of pseudotachylyte are identified on the basis of deformation texture, vein morphology, and host rock lithology: cataclasite-related (C-Pt), mylonite-related (M-Pt), and ultramylonite-related (Um-Pt). The textural and structural relationships between these pseudotachylyte veins and wall rocks indicate multiple stages of pseudotachylyte veins that formed at different times and depths.
Preliminary works have been performed by Lin et al. (2005) and Lin (2008), which have reported large volumes of coexisting C-Pt, M-Pt, and Um-Pt in cataclastic and mylonitic rocks within individual shear zones along the Woodroffe thrust. The M-Pt and Um-Pt veins contain distinct evidence of ductile deformation, including flattened and aligned fragments of host rocks that were re-oriented parallel to the foliation within the mylonite and ultramylonite, as evidenced from the continuity of the foliation between the host rock and vein fragments. These M-Pt and Um-Pt veins generally cut across the mylonitic foliation, and can locally be traced back to parent veins oriented parallel to the mylonitic foliation. These overprinting structural relationships indicate tat repeated pseudotachylyte-generating events occurred within the crystal-plastic dominated shear zone and that the pseudotachylyte veins themselves were mylonitized during ongoing plastic deformation. Here, we describe the microstructural and chemical characteristics of pseudotachylytes and discuss the processes leading to coseismic shear zone formation in the lower crust.
References:
Lin, A. et al., 2005, Propagation of seismic slip from brittle to ductile crust: Evidence from pseudotachylyte of the Woodroffe thrust, central Australia. *Tectonophysics* 402, 21-35.
Lin, A., 2008. Seismic slip in the lower crust, inferred from granulite-related pseudotachylyte in the Woodroffe thrust, central Australia. *Pure and Applied Geophysics*, 165, 215-233.

Keywords: pseudotachylyte, mylonite, ultramylonite

Structural and mineralogical characteristics of an ancient plate boundary fault in the Hidakagawa Formation, Kii Peninsula, Japan

*Takeaki Ogawa[1], Naoki Kato[1], Naoya Tonoike[1], Satoru Asayama[1], Shunya Kaneki[1], Yuki Nakano[1], Tetsuro Hirono[1]

1.Department of Earth and Space Science, Graduate School of Science, Osaka University

To understand the slip behavior of mega earthquakes along plate boundary faults, geological studies of ancient seismogenic subduction faults in onland accretionary complexes such as Shimanto have been performed in providing important information about the characteristics of the fault-zone materials. Because the trench-parallel heterogeneity in the slip behavior of subduction earthquake is important to estimate the magnitude of the rapture area in the Nankai Trough, a more investigation at various regions in the Shimanto is required.
We here targeted the mélange unit of the Hidakagawa Formation, distributed around the Mio region, Kii Peninsula, and performed structural analysis of the fault rocks on the field and laboratory-based analyses such as XRD and SEM. We found a localized slip zone accompanying the evidence of intense shearing and melting, which might corresponds to an ancient seismogenic fault in the subduction boundary.

Keywords: plate boundary fault, accretionary prism, Nankai trough

Distribution and characters of fault system in micro earthquake swarm area in central part of the Shimane Prefecture, southwest Japan

*Hideki Mukoyoshi[1], Masayuki Takeshima

1.Department of Geoscience Interdisciplinary Graduate School of Science and Engineering, Shimane University

Along a zone of central part of the Shimane prefecture to northern central part of the Hiroshima prefecture, magunitude (*M*) 5 class earthquake have occurred 6 times. In this area, numerous micro earthquakes is observed until recent days. The micro earthquake swarm zone is linearly distributed and the direction is parallel to the aftershock area of the 2000 Western Tottori earthquake (*M* 7.3). The linearly distributed micro earthquake swarm zone may reflect existence of concealed fault. However, active fault has not been reported around the zones and relationship of distribution of the micro earthquakes and geological background is also unknown. The objective of this study is to reveal the geologic structure, distribution of fault system and the characters based on the field observation on an area of the micro earthquake swarm zone.
The late Paleogene granitic rocks of the Akana granodiorite and the Ijimi granite, the Hakami volcanic rock is exposed in the study area. Basalt-andesite dikes, rhyolite dikes, and aplite is intruded into the granitic rocks.
More than 100 faults were observed in this study area. The fault plane is generally WNW strike with steeply north-dipping and NE strike with steeply south-dipping. Most of NE trending faults developed along granitic rock and dykes or granodiorite and granite. Some mm to cm thick white, light green and brown fault gouge and several cm to m thick cataclasite were observed in the faults. Fault rock of boundary fault of the Akana granodiorite and the Ijimi granite was composed of the tens of cm thick light greenish fault gouge, several m thick cataclasite, fault breccia and dozens of m of altered damaged zone. Some acidic dykes were intruded into the altered damaged zone and these dykes were not deformed. In contrast, the WNW trending faults cut the dykes and some mm to several cm thick thin fault gouges were observed within the faults. Cataclasites were not observed from the WNW trending faults.
The NE trending faults observed in this study is relatively thick with fault gouge and cataclasite. These fault plane is nearly orthogonal to the distribution direction of the micro earthquake swarms and dykes in the altered damaged zone of those faults were not deformed. These result indicates that the NE trending faults were formed in geologic period and not active at the present stress field. In contrast, WNW trending faults were developed independently of boundary of lithofacies and most of them has thin fault gouge. The orientation and occurrence of WNW trending fault are similar to the faults reported from aftershock area of the 2000 Western Tottori earthquake (Kobayashi et al., 2003; Aizawa et al., 2005). These result suggest WNW trending faults are considered as the Riedel shear planes of main fault and formed in the present stress field.

